Accepted Manuscript

Title: Stratigraphy of the Cenomanian-Turonian Oceanic Anoxic vent OAE2 in shallow shelf sequences of NE Egypt

Authors: Ahmed El-Sabbagh, Abdel Aziz Tantawy, Gerta Keller, Hassan Khozyem, Jorge Spangenberg, Thierry Adatte, Brian Gertsch

PII: S0195-6671(11)00047-4

DOI: 10.1016/j.cretres.2011.04.006

Reference: YCRES 2638

To appear in: *Cretaceous Research*

Received Date: 10 December 2009

Revised Date: 15 February 2011

Accepted Date: 18 April 2011

Please cite this article as: El-Sabbagh, A., Tantawy, A.A., Keller, G., Khozyem, H., Spangenberg, J., Adatte, T., Gertsch, B. Stratigraphy of the Cenomanian-Turonian Oceanic Anoxic vent OAE2 in shallow shelf sequences of NE Egypt, Cretaceous Research (2011), doi: 10.1016/j.cretres.2011.04.006

Stratigraphy of the Cenomanian-Turonian Oceanic Anoxic Event OAE2 in shallow shelf sequences of NE Egypt

Ahmed El-Sabbagh [a, *], Abdel Aziz Tantawy [b], Gerta Keller [c], Hassan Khozyem [d], Jorge Spangenberg [d], Thierry Adatte [d], Brian Gertsch [e]

[a] Department of Geology, Faculty of Science, Alexandria University, Alexandria 21511, Egypt
[b] Department of Geology, Aswan Faculty of Science, South Valley University, Aswan 81528, Egypt
[c] Department of Geosciences, Princeton University, Guyot Hall, Princeton, NJ 08544, USA
[d] Institut de géologie et paleontologie, Université de Lausanne, Anthropole, 1015 Lausanne, Switzerland
[e] Earth, Atmospheric and Planetary Science Department, MIT, Cambridge, MA 02139, USA

ABSTRACT

Two shallow water late Cenomanian to early Turonian sequences of NE Egypt have been investigated to evaluate the response to OAE2. Age control based on calcareous nannoplankton, planktic foraminifera and ammonite biostratigraphies integrated with $\delta^{13}C$ stratigraphy is relatively good despite low diversity and sporadic occurrences. Planktic and benthic foraminiferal faunas are characterized by dysoxic, brackish and mesotrophic conditions, as indicated by low species diversity, low oxygen and low salinity tolerant planktic and benthic species, along with oyster-rich limestone layers. In these subtidal to inner neritic environments the OAE2 $\delta^{13}C$ excursion appears comparable and coeval to that of open marine environments. However, in contrast to open marine environments where anoxic conditions begin after the first $\delta^{13}C$ peak and end at or near the Cenomanian-Turonian boundary, in shallow coastal environments anoxic conditions do not appear until the early Turonian. This delay in anoxia appears to be related to the sea level transgression that reached its maximum in the early Turonian, as observed in shallow water sections from Egypt to Morocco.

Keywords: Cenomanian-Turonian; OAE2; Shallow water sequences; Egypt

* Corresponding author: E-mail: ah.elsabbagh@gmail.com (A. El-Sabbagh)

1. Introduction

The mid-Cretaceous (120–80 Ma) represents one of the warmest periods in Earth's history (Norris et al., 2002; Gustafsson et al., 2003; Forster et al., 2007) characterized by high atmospheric CO_2 levels (Arthur et al., 1985, 1991), high tropical sea-surface temperatures accompanied by relatively low latitudinal temperature gradients (Huber et al., 2002; Norris et al., 2002; Forster et al., 2007; Pucéat et al., 2007), a high sea level (Haq et al., 1987; Hallam, 1992; Voigt et al., 2006, 2007) and faunal and floral turnovers (Jarvis et al., 1988; Hart et al., 1993; Keller et al., 2001, 2008; Leckie et al., 2002; Erba and Tremolada, 2004; Keller and Pardo, 2004; Gebhardt et al., 2010; Gertsch et al., 2010b; Linnert et al., 2010). These greenhouse conditions coincided with a worldwide pulse in the production of new oceanic crust (Sinton et al., 1998; Courtillot and Renne, 2003; Snow et al., 2005; Turgeon and Creaser, 2008; Seton et al., 2009). Within this time interval, repeated widespread deposition of organic-rich shale, associated with major $\delta^{13}C$ excursions mark perturbations in the carbon cycle and enhanced burial of ^{13}C-depleted organic carbon during five Oceanic Anoxic Events (OAEs) (e.g., Hart and Leary, 1989; Erbacher et al., 1999; Leckie et al., 2002; Pucéat, 2008).

Among these oceanic anoxic events, OAE2 represents the climax of a cycle of black shale deposition in the latest Cenomanian planktic foraminiferal *Rotalipora cushmani* Zone (e.g., Hart et al., 1993; Leckie et al., 1998; Keller et al., 2001, 2004, 2008; Keller and Pardo, 2004; Kuhnt et al., 2005; Voigt et al., 2006, 2007, 2008; Gebhardt et al., 2010). OAE2 is characterized by a ~2-3‰ positive shift in carbon isotopes and up to 6‰ in organic carbon that reflects an increase in productivity and/or carbon burial (Arthur et al., 1990; Keller et al., 2001, 2004; Kolonic et al., 2005; Jarvis

et al., 2006; Voigt et al., 2006, 2007, 2008; Mort et al., 2008; Gebhardt et al., 2010; Linnert et al., 2010).

Black organic-rich shale characterizes OAE2 in deeper waters (outer shelf-upper slope), upwelling areas and basin settings of the North Atlantic, Mediterranean and surrounding margins (Kuhnt et al., 1997; Kolonic et al., 2002, 2005; Voigt et al., 2006, 2007, 2008; Keller et al., 2008; Mort et al., 2008). However, in shallow marine platform and coastal areas (e.g., eastern Tethys) organic-rich black shales are generally absent, either because they were not deposited or not preserved (van Buchem et al., 2002; Lüning et al., 2004; Gertsch et al., 2010a). In these shallow marine settings, faunal assemblages are characterized by low diversity, sporadic occurrences and long-ranging stress resistant species that provide relatively poor age control (Keller and Pardo, 2004; Gebhardt et al., 2010; Gertsch et al., 2010a, b).

This study examines carbon isotopes, micro- and macrofossil biostratigraphies and faunal turnovers of the latest Cenomanian OAE2 in two shallow water coastal sequences (Wadi Dakhl and Wadi Feiran) of northeastern Egypt (Fig. 1). The results are correlated with published OAE2 records from other shallow water sequences in Egypt (Wadi El Ghaib, eastern Sinai, Gertsch et al., 2010a), Pueblo, Colorado (stratotype section and point, GSSP, Keller et al., 2004; Keller and Pardo, 2004), and NW Morocco (Azazoul section, Gertsch et al., 2010b, Fig. 2A). Specific objectives include: (1) stable carbon isotopes to evaluate the extend of the OAE2 $\delta^{13}C$ excursion in marine-coastal areas, (2) biostratigraphy and age control based on macrofossils and microfossils (e.g., ammonites, oysters, planktic foraminifera, calcareous nannoplankton) and (3) evaluate faunal turnovers in shallow marine sequences insofar as the sporadic fossil record permits.

2. Geological setting

During the Cenomanian-Turonian, Egypt was part of a broad Tethyan Seaway with open marine circulation to the Indo-Pacific in the east and the Atlantic-Caribbean-Pacific in the west (Fig. 2B) (Said, 1990; Lüning et al., 1998, 2004; Issawi et al., 1999). Sediment deposition in Egypt occurred mainly during the sea-level transgression that progressively advanced to the south. Carbonate deposition marks the northern deeper part of the seaway (northern Sinai and the northern part of the Western Desert), whereas to the south (central and southern Sinai and the Eastern Desert) clastic sedimentation dominates (Kerdany and Cherif, 1990; Issawi et al., 1999; El-Sabbagh, 2000, 2008; Wilmsen and Nagm, 2009; Gertsch et al., 2010a). In shallow basins of the south, episodic sea level fluctuations associated with high terrigenous influx are indicated by rapid facies changes of carbonates alternating with sandstones (Bachmann and Kuss, 1998; Lüning et al., 1998; Bauer et al., 2001, 2003).

Along the margins west and east of the Gulf of Suez rift, the Cenomanian-Turonian strata have an extensive aerial distribution and form distinct rock units lying almost directly on different horizons of the pre-Cenomanian Nubian Sandstone (Kerdany and Cherif, 1990; Issawi et al., 1999). They include beds with common to abundant macrofauna (e.g., ammonites, oysters) and intervals enriched in microfauna (e.g., foraminifera, nannoplankton) as reported in various publications (e.g., Said, 1962, 1990; Malchus, 1990; Kassab and Obaidalla, 2001; El-Sabbagh, 2008; Gertsch et al., 2010a; Nagm et al., 2010a, b).

Outcrops at Wadi Dakhl and Wadi Feiran represent parts of the margins west and east of the Gulf of Suez rift, respectively. The main bedrock outcrops are distributed in two major highly fractured elongated platforms running parallel to the Gulf of Suez (Said, 1962, 1990; Kerdany and Cherif, 1990). Wadi Dakhl is located in the southern

part of the Southern Galala Plateau west of the Gulf of Suez with the Wadi Dakhl section located north of Bir Dakhl, about 30 km southwest of the Monastery of St. Paul (32°25\ E, 28°41\ N, Fig. 1). Wadi Feiran trends east-west in the southwestern Sinai and the section is located near the village of Mukattab, about 18 km from the Feiran traffic station at the road entrance to the Monastery of St. Catherine (33°31\ E, 28°47\ N).

3. Methods

The Wadi Dakhl and Wadi Feiran sections were examined in the field for lithological changes, burrows, macrofossils, hardgrounds and erosion surfaces, which were described, measured and sampled. A total of 119 rock samples were collected at an average of 30-50 cm intervals for the Wadi Dakhl outcrop and 57 rock samples for the Wadi Feiran outcrop at intervals of about 25 cm. At Wadi Dakhl, macrofossil assemblages were collected throughout the sequence wherever present. At Wadi Feiran only few macrofossils were observed.

In the laboratory, sediment samples were processed for foraminiferal analysis using standard methods (Keller et al., 1995). Planktic and benthic foraminifera were analyzed in the >63 μm size fraction, mounted on microslides and identified. Planktic foraminifera are generally rare, though common in some intervals in both sections. Benthic foraminifera are common to abundant. Quantitative estimates of foraminifera were obtained from at least 100 planktic specimens, and up to 600 benthic specimens. Identification of planktic and benthic species follows that of Cushman (1946), Omara (1956), Sliter (1968), Robaszynski and Caron (1979, 1985), and Bolli et al. (1994). Preservation of foraminiferal tests is good to moderate.

Calcareous nannofossils were processed by standard smear slide preparation from raw sediment samples as described by Perch-Nielsen (1985). Smear slides were

examined using a light photomicroscope with 1000x magnification. Each slide was observed under cross-polarized light. Preservation and abundance of nannofossils are moderate to poor throughout the Wadi Feiran section. Calcareous nannofossil species abundances were semiquantitatively evaluated as follows: common: >1 specimen per field of view (FOV); few: 1 specimen per 1–10 FOV; rare: 1 specimen per >10 FOV.

Carbon isotope composition of bulk rock carbonates was determined using a Thermo Fisher carbonate-preparation device and GasBench II connected to a Thermo Fisher Delta Plus XL continuous He flow isotope ratio mass spectrometer (IRMS). CO_2 extraction was done with 100% phosphoric acid at 70°C for calcite and 90°C for dolomite. The stable carbon isotope ratios are reported in the delta (δ) notation as the permil (‰) deviation relative to the Vienna-Pee Dee belemnite standard (VPDB). Analytical uncertainty (2 σ), monitored by replicate analyses of the international calcite standard NBS-19 and the laboratory standards Carrara Marble and Binn Dolomite was better than ±0.05‰ for $\delta^{13}C$.

4. Lithology

At Wadi Dakhl and Wadi Feiran, the Cenomanian-Turonian sequences are composed of siliciclastic sediments in the lower part, mixed siliciclastic carbonates in the middle part, and mostly carbonates in the upper part (Figs. 3, 4). Different lithostratigraphic schemes have been proposed to describe the Cenomanian-Turonian deposits in the northern Eastern Desert, Gulf of Suez and western Sinai despite lithologic and faunal similarities (e.g., Cherif et al., 1989; Kerdany and Cherif, 1990; Kora et al., 2001; El-Sabbagh, 2008; Wilmsen and Nagm, 2009). As a result, the Cenomanian-Turonian deposits of the Wadi Dakhl and Wadi Feiran sections were

included in the Raha (early-late Cenomanian), Abu Qada (late Cenomanian-early Turonian) and Wata (late Turonian) Formations (Figs. 3, 4).

The Raha Formation (Ghorab, 1961) is well represented in the Wadi Dakhl section by sandstone, shale, marl, dolomite and limestone (Fig. 3) that reflect the first shallow marine transgression in northeastern Egypt during the Cenomanian (Kerdany and Cherif, 1990; Issawi et al., 1999). Around the Gulf of Suez, the top of a sandstone interval (i.e., the Mellaha Sand Member of Ghorab, 1961) marks the Raha/Abu Qada transition (Cherif et al., 1989; Kora et al., 2001; El-Sabbagh, 2008). At the Wadi Dakhl section, sandstone deposition ends at 33.7 m, which may represent the Raha/Abu Qada boundary. The lower part of the Raha Formation is poorly fossiliferous with oysters, trigonid bivalves, gastropods and a few bioturbated levels. The middle part contains more common oysters, gastropods, bivalves, ammonite, rudists and echinoids, whereas the sandstones of the upper part are largely devoid of macrofossils.

The Abu Qada Formation (Ghorab, 1961) is well developed in the Wadi Dakhl and Wadi Feiran sections (Figs. 3, 4) and consists of shales, marls, nodular marls, limestones and oyster-rich limestone beds. Ammonites are rare in the Wadi Feiran section, but macrofossils are common to abundant in the Wadi Dakhl section, including ammonites, gastropods, bivalves, rudists, echinoids, corals, sponges and ichnofossils. The Wata Formation (Ghorab, 1961) in Wadi Dakhl is represented by a carbonate facies consisting of limestone, marly limestone and shales with common ammonites, bivalves, gastropods and echinoids (Fig. 3).

The Wadi Dakhl section spans from the lower Cenomanian to the upper Turonian. The basal 9.0 m consist of sandstone intercalated with sandy silty shale in the lower and upper parts. Between 9.0-24.7 m, sediments consist of alternating marl (Fig. 3B), dolomite, dolomitic limestone, shale and silty-sandy shale layers. A unique 0.5 m

thick oyster bed is present at 18.8 m (Fig. 3). A clastic interval between 24.7-36.1 m consists of alternating sandstone, shale, silty sandy shale, a thin marl bed at 29.3 m and a thick shale layer at the top. Oyster-rich limestone and marly limestone layers (36.1-42.6 m) overlie this interval and are intercalated with marl and shale layers. Above is a thick shale layer followed by a 1.0 m thick oyster bed and an interval of alternating shale, marl, marly limestone and thin dolomite layers (42.6-55.0 m). Lithologies between 55.0-60.3 m are dominated by limestone, marly limestone and thin shale layers with common ammonites and echinoids. A disconformity is indicated at the top of this unit by the strongly bioturbated limestone followed by a red laminated shale layer (1.8 m thick) that marks the transition to a poorly fossiliferous interval (62.1-66.6 m) of silty-sandy shale, sandstone, shale and marl layers (Fig. 3). Near the top of the section is a thick fossiliferous marly limestone, partly dolomitic (66.6-76.6 m) with a 0.8 m thick shale bed. Shale, marly and partly dolomitic limestones mark the uppermost part of the section.

The Wadi Feiran section outcrops in a cliff and spans the late Cenomanian to early Turonian (Fig. 4). The lower part of the section (0-2.7 m) consists of alternating marl and shale layers with thin nodular marly limestone (10 cm thick) and oyster (20 cm thick) beds. Marls contain rare nodules and are poorly fossiliferous. Rhythmically bedded thin marl and limestone layers overlie this interval (2.7-5.0 m). A thick marly limestone bed (5.0-11.3 m) terminates at a 1.1 m thick oyster bed with an erositional surface at the top (Fig. 4). Between 12.4-14.0 m is a fossiliferous dolomitic limestone layer with multiple hardground surfaces indicating nondeposition and/or erosion (reef facies). Alternating marls and shales with ammonites (14.0-15.5 m) underlie a thick bed of highly fossiliferous (bioclastic) limestone (15.5-19.9 m). This unit terminates at a 0.5 m thick marly limestone layer containing rare echinoids. Above is a red laminated shale

layer (0.4 m thick). The top of the section (20.8-23.0 m) consists of a thick marl layer with a 0.3 m thick marly limestone layer in the middle part (Fig. 4).

5. Isotope stratigraphy

In shallow water sequences, carbonates are likely to undergo diagenesis that alters the primary isotopic signals and limits their role in paleoenvironmental interpretations (Jenkyns et al., 1994; Schrag et al., 1995). Diagenesis strongly affects oxygen isotopes by recrystallization and/or interstitial fluids, which leads to significant lowering of $\delta^{18}O$ values and obliterates the original seawater temperature signals, though trends tend to be preserved (Jenkyns et al., 1994; Mitchell et al., 1997; Paul et al., 1999). In contrast, $\delta^{13}C$ values are little affected by diagenesis due to the low carbon content of pore waters (Schrag et al., 1995), except in sediments influenced by organogenic carbon incorporation (Marshall, 1992). Carbon isotopes therefore closely track environmental changes.

Wadi Feiran: In the basal part of the Abu Qada Formation, $\delta^{13}C$ data show low values (-1.4-1.5‰) with a drop to -0.3‰ just below an oyster bed (1.9 m), followed by a sharp increase to 2.9‰ in a 0.2 m thick oyster bed and a further increase to 4.6‰ at 3 m (Fig. 5A). This $\delta^{13}C$ shift marks the global OAE2 excursion and the first (peak 1) of two $\delta^{13}C$ maxima, as observed worldwide (e.g., Kuhnt et al., 1997, 2005; Keller et al., 2001, 2004, 2008; Leckie et al., 2002; Kolonic et al., 2005; Jarvis et al., 2006; Voigt et al., 2006, 2007, 2008; Gebhardt et al., 2010; Gertsch et al., 2010a, b; Linnert et al., 2010). After the first peak, $\delta^{13}C$ values drop to 2.5‰ then gradually increase to 4.5‰ at 6.5 m, which probably marks the second peak of the global $\delta^{13}C$ excursion (Fig. 5A). $\delta^{13}C$ values remain relatively high and steady up to 20.6 m where they gradually decrease to 2‰ in the upper part of the Abu Qada Formation.

Wadi Dakhl: Samples that contain sufficient carbonate for stable isotope analysis are relatively few at the shallower Wadi Dakhl section (Fig. 5B). In the middle part of the Raha Formation (18.5 m) the $\delta^{13}C$ curve shows low values (0.19‰). An increase to 1.4‰ occurs in a 0.5 m thick oyster bed (18.8-19.3 m), followed by a decrease to -0.3‰ in the overlying marl (21.3 m). Between 21.3 m to 36.0 m carbonate values are too low for stable isotope analysis. In the lower part of the Abu Qada Formation (36-50.4 m), $\delta^{13}C$ values fluctuate between 0.4 and 1.9‰ with values up to 2.2‰ at 41 m. Between 50.4-55.1 m, no samples are available (dashed line in $\delta^{13}C$ curve, Fig. 5B). Above this level, $\delta^{13}C$ values reach 4.3‰ and mark the upper part of the OAE2 excursion below the C/T boundary. Just above the C/T boundary, an abrupt drop in $\delta^{13}C$ to -1.2‰ at 60 m marks a major hiatus with early Turonian sediments above it. The absence of the characteristic two $\delta^{13}C$ peaks and prolonged plateau indicates that this hiatus spans most of the OAE2 excursion. In the upper Turonian Wata Formation, $\delta^{13}C$ values fluctuate between -0.4-2.4‰. The relatively small-scale cyclical oscillations in this interval may be largely the result of lithological changes (Paul et al., 1999; Keller et al., 2001; Voigt et al., 2006).

6. Biostratigraphy

6.1. Ammonites

In shallow water Cenomanian-Turonian sequences of the southern Tethys, ammonites offer good age control and regional correlations (Robaszynski and Caron, 1995; Hardenbol et al., 1998). Low diversity and endemism has led to a number of regional ammonite biozonations, including Egypt (Table 1). These biozonations have been widely discussed (Kora and Hamama, 1987; Kassab, 1991, 1994, 1999; Kassab and Ismael, 1994; El-Sabbagh, 2000, 2008; Kassab and Obaidalla, 2001; El-Hedeny,

2002; Zakhera and Kassab, 2002; Nagm et al., 2010a, b) and correlated with the Pueblo, Colorado, stratotype section and point (GSSP) based on carbon isotope stratigraphy (e.g., Gertsch et al., 2010a, b).

6.1.1. Neolobites vibrayeanus interval zone (Zone C1)

Zone C1 is defined by the total range of the zonal marker *N. vibrayeanus* (Fig. 6). In the Wadi Dakhl section occurrences of the index species were observed between 21.0-23.4 m, which tentatively identify the base of zone C1 (Fig. 7). Associated with these occurrences is the oyster *Ilymatogyra* (*Afrogyra*) *africana*, a characteristic early late Cenomanian species of Egypt (Malchus, 1990; El-Sabbagh, 2000, 2008). In the Wadi El Ghaib section, zone C1 spans up to the first appearance of *Vascoceras cauvini*, which is coincident with the first peak of the $\delta^{13}C$ shift at 4.5‰ (Gertsch et al., 2010a). At Wadi Dakhl, C1 also spans the interval below the $\delta^{13}C$ excursion, though the C1/C2 boundary is uncertain because the $\delta^{13}C$ shift and most of the plateau are missing (Fig. 7). Zone C1 was not sampled in the Wadi Feiran section.

In Egypt, zone C1 is generally confined to the upper part of the Raha Formation (Abdel-Gawad, 1999; Kassab and Obaidalla, 2001; El-Sabbagh, 2008; Gertsch et al., 2010a). However, in the field the boundary placement between the Raha and Abu Qada Formations is uncertain. The Mellaha Sand Member of Ghorab (1961) is considered a marker horizon. However, a sandstone unit is not a unique marker in shallow water sequences that frequently contain sandstones. In the absence of distinct lithologic markers, the boundary between the Raha and Abu Qada Formations remains unknown. For these reasons, we tentatively identify the upper part of the Raha Formation as equivalent to zone C1.

6.1.2. Vascoceras cauvini interval zone (Zone C2)

Zone C2 is defined by the first occurrence (FO) of the zonal marker *V. cauvini* at the base and/or the last occurrence (LO) of *N. vibrayeanus*. The top of zone C2 is marked by the LO of *V. cauvini* and/or the FO of *V. proprium,* an early Turonian ammonite that marks the Cenomanian-Turonian (C/T) boundary. In Egypt, the base of zone C2 coincides with the trough between the $\delta^{13}C$ excursion peak 1 and peak 2, whereas the top coincides with the end of the $\delta^{13}C$ plateau at or near the C/T boundary (Gertsch et al., 2010a).

At the Wadi Dakhl section, the $\delta^{13}C$ excursion and plateau are mostly missing due to one or more hiatuses. Only a short interval of high $\delta^{13}C$ values (3.8-4.3 ‰) is present and probably represents part of the plateau. In this interval *V. cauvini* is present and marks zone C2 (Figs. 6, 7). The oyster *Exogyra* (*Costagyra*) *olisiponensis,* which marks the latest Cenomanian in the Tethys seaway (Kennedy et al., 1987; Meister et al., 1992; Chancellor et al., 1994; Kassab and Obaidalla, 2001; Wilmsen and Nagm, 2009), was observed below the FO of *V. cauvini*. Above this interval, $\delta^{13}C$ values abruptly drop to <1‰ and indicate a hiatus at or near the C/T boundary (Fig. 7). Above the hiatus, the early Turonian ammonites *V. proprium* and *V. durandi* are present. Below the interval of high $\delta^{13}C$ values the onset of the $\delta^{13}C$ excursion and maximum values (peak 1 and peak 2) are missing, which indicates another hiatus.

At Wadi Feiran, the base of C2 can be tentatively inferred by the rare occurrence of *V. cauvini*, which coincides with the upper part of the $\delta^{13}C$ plateau (Fig. 8). The characteristic ammonites that define the C/T boundary were not observed, although Kassab and Obaidalla (2001) reported them earlier. The C/T boundary was therefore placed at the end of the $\delta^{13}C$ plateau excursion, coincident with the position of this boundary event globally.

6.1.3. Vascoceras proprium total range zone (Zone T1)

Zone T1 is defined by the total range of the zonal index species *V. proprium*. These globose vascoceratids (Fig. 6) are good biostratigraphic indicators for the early Turonian in the southern Tethys (Hardenbol et al., 1993; Robaszynski and Gale, 1993; Chancellor et al., 1994). At Wadi Dakhl, *V. proprium* was observed along with *V. durandi* in a very short interval (59.0-60.4 m) above the hiatus evident in the $\delta^{13}C$ curve (Fig. 7). This indicates that most of zone T1 is missing. At Wadi Feiran, the zone T1 index species was not observed. *V. proprium* is common in the early Turonian *Pseudoaspidoceras flexuosum* Zone in the Tethyan realm (Meister and Rhalmi, 2002; Meister and Abdallah, 2005) and US Western Interior (Kennedy et al., 1987; Kennedy and Cobban, 1991). Zone T1 is thus considered equivalent to the *P. flexuosum* Zone and probably the *Watinoceras devonense* Zone (Table 1).

6.1.4. Choffaticeras segne total range zone (Zone T2)

Zone T2 is defined by the total range of the nominate species (Fig. 6). At Wadi Dakhl, zone T2 is recognized between 60.4-66.6 m in the upper part of the Abu Qada Formation, and at Wadi Feiran between 20.8-23.0 m. In both sections zone T2 coincides with low $\delta^{13}C$ values (Figs. 7, 8).

6.1.5. Coilopoceras requienianum total range zone (Zone T3)

Zone T3 is defined by the total range of the zonal index species. *Coilopoceras requienianum* was observed in the Wadi Dakhl section (Fig. 6) with the first appearance about 4 m above *Ch. segne*. Therefore, the T2/T3 boundary is tentatively identified (dashed interval, Fig. 7). The last occurrence was observed at 76.6 m. Zone T3 and thus

spans an interval from 70.6-76.6 m at Wadi Dakhl. *Coilopoceras requienianum* is a well-known late Turonian ammonite index species (e.g., Cobban and Hook, 1980; Wright et al., 1984; Nagm et al., 2010a, b).

6.2. Planktic foraminifera

Planktic foraminiferal assemblages are present only in sporadic intervals and rotaliporid index species generally rare or absent in the shallow water sequences of Egypt (Cherif et al., 1989; Shahin and Kora, 1991; Kora et al., 1994; Gertsch et al., 2010a). Relative age interpretations can be made based on these sporadic assemblages and integration with calcareous nannofossils and carbon isotope stratigraphies.

Wadi Dakhl: In this section, the Cenomanian-Turonian planktic foraminiferal assemblages range from few to common (Fig. 7). In the marl and shale layers below the high $\delta^{13}C$ values, heterohelicids, hedbergellids and globigerinellids are sporadically common and whiteinellids are present (e.g., *Praeglobotruncana stephani, Dicarinella algeriana).* This interval is tentatively placed in the *Rotalipora cushmani* Zone. *Whiteinella archeocretacea* are present between 49.2-54.9 m, an interval that is tentatively placed in the *W. archeocretacea* Zone (Fig. 7). Above this interval, high $\delta^{13}C$ values indicative of the OAE2 plateau indicates the upper part of the *W. archeocretacea* Zone, although the interval is barren (Keller and Pardo, 2004; Keller et al., 2008; Caron et al., 2006). *Globigerinelloides bentonensis*, which generally disappears above the $\delta^{13}C$ excursion peaks (Keller et al., 2001; Keller and Pardo, 2004), is absent. This indicates that the lower part of the OAE2 $\delta^{13}C$ excursion is missing at the Wadi Dakhl section. The uppermost planktic foraminiferal assemblage occurs in the shale and limestone layers between 59.0-61.0 m above the high $\delta^{13}C$ values. This assemblage contains

abundant heterohelicids and whiteinellids, which is generally indicative of the early Turonian, though no zonal index species are present.

Wadi Feiran: In this section, planktic foraminifera range from few to common with the first sporadic assemblages of heterohelicids, hedbergellids, whiteinellids and dicarinellids in marl, shale and marly limestone layers between 0-10.3 m. (Fig. 8). *Whiteinella archeocretacea* first appears at 1.5 m, near the onset of the $\delta^{13}C$ excursion, as also observed in the Wadi El Ghaib section in the eastern Sinai (Gertsch et al., 2010a) and elsewhere (Nederbragt and Fiorentino, l999; Keller et al., 2001, 2008; Leckie et al., 2002; Keller and Pardo, 2004; Caron et al., 2006; Gebhardt et al., 2010; Gertsch et al., 2010b). Rotaliporids are absent in this shallow water environment.

The base of the *W. archeocretacea* Zone is defined globally by the extinction of all *Rotalipora* species, including the index species *R. cushmani* (Caron, 1985; Robaszynski and Caron, 1995). This extinction datum occurs in the trough between $\delta^{13}C$ peaks 1 and 2 (e.g., Keller et al., 2001, 2008; Leckie et al., 2002; Kuhnt et al., 2005; Gebhardt et al., 2010; Gertsch et al., 2010b), except for the Pueblo stratotype section, where the *R. cushmani* extinction coincides with the $\delta^{13}C$ peak 1 as a result of condensed sedimentation (Keller and Pardo 2004). At Wadi Feiran, we tentatively place the *R. cushmani/W. archeocretacea* Zone boundary in the trough (4.75 m) between the two $\delta^{13}C$ peaks and just below the FO of *D. imbricata,* as also observed in the Pueblo stratotype section (Fig. 8). Above the OAE2 $\delta^{13}C$ excursion (21.1-21.8 m), a relatively diverse planktic foraminiferal assemblage of heterohelicids, hedbergellids and whiteinellids is indicative of early Turonian age, though the index species *Helvetoglobotruncana helvetica* is absent. The C/T boundary is tentatively placed at the end of the $\delta^{13}C$ excursion plateau, correlative with the Pueblo stratotype section and

elsewhere (Hart et al., 1993; Keller and Pardo, 2004; Voigt et al., 2006, 2007; Gebhardt et al., 2010; Gertsch et al., 2010b).

6.3. Calcareous Nannofossils

Calcareous nannofossils at Wadi Feiran are generally rare, poorly preserved and limited to distinct lithostratigraphic units (Fig. 8). Sixty-three species attributable to 21 genera were identified, including the index taxa, which allow reasonably good biostratigraphic resolution (Fig. 9). This study mainly follows the standard cosmopolitan zonations of Sissingh (1977) and Perch-Nielsen (1979, 1985) and incorporates additional bioevents from Bralower (1988) and Burnett (1998). Two nannofossil zones (CC10 and CC11) and three subzones (CC10a-c) have been identified and correlated regionally (e.g., Sinai, Jordan, Tunisia, Morocco, Table 2).

Zone CC10 spans the late Cenomanian (Perch-Nielsen, 1985) and is defined by the interval from the first occurrence (FO) of *Lithraphidites acutus* and/or FO of *Microrhabdulus decoratus* to the FO of *Quadrum gartneri.* Manivit et al. (1977) and Perch-Nielsen (1985) subdivided Zone CC10 into a lower CC10a, or *Microstaurus chiastius* subzone, based on the last Burnett (1998) divided the same interval into four zones: Zone UC3 - Zone UC6 (Table 2). Recently, Tantawy (2008) subdivided Zone CC10 into three subzones (a, b and c) based on the successive last occurrences of *Axopodorhadbus albianus* and *Helenea (Microstaurus) chiastia* (Fig. 8, Table 2). These events order consistently relative to other marker species and provide reliable indices (Bralower, 1988).

At the Wadi Feiran section, subzone CC10a spans the basal 3.8 m of the Abu Qada Formation (Fig. 8). Preservation in the lower part of this subzone is generally poor with low abundances and species richness. Subzone CC10b is recognized between 3.8-

8.3 m of the Abu Qada Formation. The base of this subzone occurs just above the $\delta^{13}C$ excursion peak 1, whereas the top lies above peak 2. The same correlation was observed in the Tarfaya basin, southern Morocco (Tantawy, 2008). Subzone CC10c is 11.6 m thick at Wadi Feiran and occupies the upper part of the Abu Qada Formation. Near the top of the section nannofossil preservation is poor and most samples are barren. The top of CC10c coincides with the end of the $\delta^{13}C$ plateau at or near the C/T boundary (Fig. 8). Subzones CC10b and CC10c correspond to Zones UC5 and UC6, respectively, of Burnett (1998).

Zone CC11 spans the Early and Middle Turonian (Perch-Nielsen, 1985) and is defined by the interval from the FO of *Quadrum gartneri* at the base to the FO *Eiffellithus eximius* (e.g., Cepek and Hay, 1969; Perch-Nielsen, 1985) and/or FO of *Lucianorhabdus maleformis* (e.g., Sissingh, 1977) at the top. Zone CC11 corresponds to Zone UC7 of Burnett (1998) and spans the uppermost part of Abu Qada Formation (Fig. 8). Preservation is poor and only 2 species are present. The base of CC11 (FO *Q. gartneri*) approximates the C/T boundary (Birkelund et al., 1984; Perch-Nielsen, 1985; Robaszynski et al., 1990; Nederbragt and Fiorentino, 1999). In the Tarfaya basin, southern Morocco, this level is observed near the top of the $\delta^{13}C$ plateau, about 45 cm below the FO of *Helvetoglobotruncana helvetica*, which approximates the C/T boundary based on planktic foraminifera (Keller et al., 2008; Tantawy, 2008; Gertsch et al., 2010b). In contrast, Bralower (1988) and Bralower et al. (1995) noticed *Quadrum gartneri* below the C/T boundary (their IC48 Zone), whereas others placed the FO of this species in the early Turonian (e.g., Burnett, 1998; Luciani and Cobianchi, 1999; Lees, 2002) (Table 2).

7. Paleoenvironment

7.1. Microfossils as environmental proxies

7.1.1. Planktic foraminifera

In shallow environments, planktic foraminifera reflect high stress conditions by generally low diversity, dwarfing and sporadic presence. In Wadi Dakhl only a narrow interval of the OAE2 $\delta^{13}C$ excursion is preserved due to erosion. No planktic foraminifera are present in this interval (Fig. 7). Immediately below is a low diversity assemblage of whiteinellids, heterohelicids, globigerinellids and hedbergellids that indicates a shallow environment. During the late Cenomanian (13-45 m) only 2 to 5 planktic foraminiferal species are sporadically present and reflect high stress conditions. In the interval above the $\delta^{13}C$ excursion, high stress conditions are indicated by the presence of only *Heterohelix* species and *W. baltica*. *Heterohelix* generally dominates nearshore assemblages in areas with salinity or oxygen fluctuations (e.g., Nederbragt, 1991, 1998; Premoli Silva and Sliter, 1999; Keller and Pardo, 2004; Pardo and Keller, 2008; Gebhardt et al., 2010), and in upwelling areas, such as Tarfaya, Morocco (Keller et al., 2008; Gertsch et al., 2010b). Planktic foraminifera reappear above the hiatus that spans most of the $\delta^{13}C$ excursion, but are absent in red shale that marks anoxic conditions during the early Turonian. It is well known that in shallow water facies organic matter is not preserved (e.g., oxidized), and, consequently, black shale is replaced by red shale (e.g., Voigt et al., 2006, 2007; Keller et al., 2008; Gertsch et al., 2010a, b).

At Wadi Feiran, the OAE2 $\delta^{13}C$ excursion interval is relatively complete (Fig. 8). Planktic foraminiferal assemblages below the $\delta^{13}C$ peak 1 consist of low oxygen and low salinity tolerant species (e.g., heterohelicids, hedbergellids, whiteinellids and guembelitrids) that reflect nutrient-rich, dysoxic conditions in a coastal environment. The low salinity tolerant hedbergellids (e.g., *Hedbergella delrioensis*, *H. planispira*),

low oxygen tolerant heterohelicids (e.g., *Heterohelix reussi*, *H. moremani*) and disaster opportunist *Guembelitria cenomana* are among the last survivors in shallow inner neritic environments (Hart, 1980, 1999; Leckie, 1987; Leckie et al., 1998, 2002; Keller and Pardo, 2004; Pardo and Keller, 2008; Keller and Abramovich, 2009). Above the $\delta^{13}C$ peaks 1 and 2, planktic foraminifera are absent, except for one isolated occurrence of *G. cenomana* and *D. algeriana*. This absence coincides with very a shallow water environment and consequently extreme stress conditions, as indicated by oyster beds and bioclastic limestones (Fig. 4). Planktic foraminifera reappear only above the $\delta^{13}C$ excursion in the early Turonian, similar to Wadi Dakhl (Figs. 7, 8), and are absent in the red layer that represents anoxic conditions.

7.1.2. Benthic foraminifera

Late Cenomanian to early Turonian benthic foraminiferal assemblages in the Wadi Feiran and Wadi Dakhl sections are more diverse and abundant than planktic species, which reflects the shallow water environment (Figs. 8, 10). Benthic foraminiferal assemblages are dominated by low oxygen tolerant agglutinated (e.g., *Ammobaculites, Haplophragmoides, Spiroplectammina, Cribrostomoides, Thomasinella*) and hyaline species (e.g., *Coryphostoma plaitum*, *Praebulimina aspera*, *Pyramidina prolixa*, *P. nannina*, *Neobulimina albertensis*, *Fursenkoina nederi*, *Gavelinella sandidgei*) (Murray, 1973). Within these assemblages, infaunal species (deposit feeders that profit from high food availability) are more abundant than epifaunal species, which indicates dysoxic seafloor conditions (Jarvis et al., 1988; Hart et al., 1993; Koutsoukos et al., 1990; Perty and Lamolda, 1996; Gebhardt et al., 2010). Benthic foraminifera are nearly absent during the $\delta^{13}C$ plateau (oyster and bioclastic limestones) and in the early Turonian red shale that reflects delayed anoxic conditions.

7.1.3. Calcareous nannofossils

The composition and distribution of nannofossil taxa are generally indicative of paleoecological and paleoenvironmental conditions (e.g., nutrient supply, surface sea water temperature, water depth). However, the effects of diagenetic processes and poor preservation strongly affect the original assemblages (Fig. 9). Effects of dissolution are indicated by high abundance of dissolution-resistant species, such as *Watznaueria barnesae* and *Eprolithus floralis* (Roth and Krumbach, 1986; Erba et al., 1992) and rare occurrence of solution-susceptible species (e.g., *Eiffellithus* species, *Tranolithus phacelosus, Prediscosphaera spinosa* (Thierstein, 1980; Roth and Krumbach, 1986; Paul et al., 1999; Linnert et al., 2010).

Watznaueria barnesae, which is common in the Late Cenomanian CC10a, b subzones, is widely used as a preservation indicator. Roth and Krumbach (1986) and Tantawy (2008) pointed out a good linear correlation between diversity and relative abundance of *W. barnesae*, although ecological factors may also have affected the distribution (Eshet and Almogi-Labin, 1996; Bauer et al., 2001). *Eprolithus floralis* shows an increased in abundance at the topmost part of CC10a and lower CC10c (Fig. 8). This species is relatively resistant to dissolution (e.g., Thierstein, 1980; Roth and Krumbach, 1986; Bralower, 1988; Linnert et al., 2010), and high abundance around the C/T boundary is at least partly a preservational artifact. Similar preservational trends and low diversity in Cenomanian–Turonian nannofossil assemblage have been observed regionally (e.g. Sinai: Bauer et al., 2001, 2003; Jordan: Schulze et al., 2004; Morocco, Tantawy, 2008; Gertsch et al., 2010b).

In the Wadi Feiran section, calcareous nannofossils suggest that surface waters were probably cooler during deposition of the lower part of Abu Qada Formation and

warmer in the upper part. This is indicated by the higher abundance of *E. floralis*, *Biscutum constans* and *Zeugrhabdotus* species in the upper CC10a and lower CC10c subzones (e.g., Roth and Krumbach, 1986; Premoli Silva et al., 1999; Mutterlose and Kessels, 2000; Mutterlose et al., 2005). Abundant *E. floralis* was previously interpreted as a characteristic of high latitudes and colder and/or lower salinity water (Roth and Krumbach, 1986; Bralower, 1988). Lamolda et al. (1994) observed the maximum abundance in the marl beds at Dover to coincide with less negative $\delta^{18}O$ values, and hence climate cooling. The tropical *Watznaueria barnesae* is common in most low to mid latitude Cretaceous assemblages but absent from high latitudes in the Cretaceous (Bukry, 1973; Thierstein, 1981; Shafik, 1990; Watkins et al., 1996; Lees, 2002; Tantawy, 2008). *Rhagodiscus* spices, which are considered a paleotemperature proxy indicative of warm water conditions (Mutterlose, 1989), are rarely present in the lower part of the section (Fig. 8).

Common *Zeugrhabdotus erectus*+spp.*, Eprolithus floralis*, *Biscutum constans*, and few *Rhagodiscus asper*/*splendens* in the lower half of the section (Figs. 8, 9) are interpreted as indicators of high surface-water productivity in upwelling regions (Roth, 1981; Roth and Krumbach, 1986; Erba, 1987; Erba et al., 1992; Mutterlose et al., 1994; Premoli Silva et al., 1999; Howe et al., 2000; Linnert et al., 2010). In the Wadi Feiran section, common *Eprolithus floralis* and *Zeugrhabdotus* species in association with oyster-rich limestone may reflect eutrophic conditions (e.g., Roth and Krumbach, 1986; Premoli Silva et al., 1999).

High abundance of the nannofossil *Broinsonia* characterizes neritic chalk seas in SE Europe, Texas and the south of France (Roth and Bowdler, 1981; Roth and Krumbach, 1986). Bralower (1988) observed high abundance of this taxon in upper Cenomanian samples from England, Germany and N. America and interpreted this as

indicating shallow water, reduced salinity or high fertility. Linnert et al. (2010) confirmed high abundance in late Cenomanian, but recorded low abundance and hence low fertility during the OAE2 interval. In the Sinai Wadi Feiran section, the shallow water depth is probably the main factor controlling the distribution of *Broinsonia* species, as well as the low diversity and abundance of other calcareous nannofossils.

7.1.4. Oyster biostromes

Biotic stressed conditions in the Wadi Dakhl and Wadi Feiran sections are also indicated by the presence of oyster-rich limestone layers that form tabular oyster biostromes as a result of high nutrient flux and rising sea level (Glenn and Arthur, 1990; Abed and Sadaqh, 1998; Dhondt et al., 1999; Pufahl and James, 2006). In the studied sections and through North Africa, oyster biostromes are commonly associated with the onset of the $\delta^{13}C$ excursion (Gertsch et al., 2010a, b). Oysters are efficient filter feeders, tolerate a wide range of environmental conditions and can respond quickly to environmental perturbations. They typically occur in high energy, shallow (<20 m) and faunally restricted environments with low salinity, mesotrophic nutrient levels and turbid water column (Pufhal and James, 2006). Such environments are generally unfavorable for planktic and most benthic foraminifera and explain their absence during the $\delta^{13}C$ plateau.

8. Late Cenomanian OAE2

The severity of the late Cenomanian oceanic anoxia (i.e., black shale deposition) in the water column depends largely on distance to the coast and water depth, terrestrial influx, marine primary productivity, organic matter preservation, oxidation in the water column, and rates of sedimentation (Pedersen and Calvert, 1990; Canfield, 1994; Arthur

and Sageman, 1994). Deeper basins near upwelling areas (i.e., typical anoxic settings; e.g., Tarfaya basin, Morocco) reveal very high sedimentation rates and organic contents (Kuhnt et al., 2005; Kolonic et al., 2005; Keller et al., 2008; Mort et al., 2008). Shallower middle shelf sequences of the U.S. Western Interior at Pueblo, England, Croatia, Portugal, Italy and Spain reveal higher terrigenous influx and lower organic contents (Hart et al., 1993, 2008; Drzewiecky and Simo, 1997; Sageman et al., 1998; Davey and Jenkyns, 1999; Gale et al., 2000; Keller et al., 2004; Keller and Pardo, 2004; Parente et al., 2007; Gebhardt et al., 2010). Among these well-known shelf settings, e.g., in southern England, Jarvis et al. (1988) suggested that organic matter preservation and reductions in microfaunal assemblages (planktic and benthic foraminifera and nannofossils) indicate dysoxic but never anoxic, brackish and mesotrophic conditions during the OAE2. However, Gale et al. (2000) argued, largely on the basis of macrofauna and trace fossil evidences, that there was not even dysaerobic and that diversity reductions were due to oligotrophic nutrient levels.

8.1. OAE2 in shallow near-shore areas

Paleoenvironmental reconstructions for the Cenomanian-early Turonian of Egypt suggest that there was no significant carbonate platform at that time (Lüning et al., 1998, 2004). During the late Cenomanian, shallow subtidal, calcareous deposits covered almost the entire Sinai (Cherif et al., 1989; Kora et al., 1994; Lüning et al., 1998; Bauer et al., 2003) and Eastern Desert (Bandel et al., 1987; Kuss, 1992; Kassab, 1994). In the northern Sinai, shoal carbonates were attached to the shelf edge (Kuss and Bachmann, 1996), whereas in the southern Sinai and Eastern Desert, a thin belt of sandstones interfingered with fluvial deposits (Bandel et al., 1987; Kuss and Bachmann, 1996). At Wadi Dakhl and Wadi Feiran, the Cenomanian-Turonian sequences reflect a

typical shallow near-shore environment deepening with the late Cenomanian to early Turonian sea level rise as indicated by dominant carbonate deposition (Figs. 3, 4). Such shallow marine environments are often characterized by high nutrients due to terrigenous runoff and low salinity due to fresh water influx (Keller et al., 2004; Keller and Pardo, 2004; Gertsch et al., 2010a, b).

In this shallow inner neritic depositional environment of Egypt, the OAE2 $\delta^{13}C$ excursion shows characteristics similar to the GSSP section at Pueblo (Leckie et al., 2002; Keller and Pardo, 2004; Caron et al., 2006; Gertsch et al., 2010a), as well as deeper marine sequences of Tunisia and Morocco (Accarie et al., 1996; Nederbragt and Fiorentino, 1999; Kolonic et al., 2005; Caron et al., 2006; Voigt et al., 2006, 2007; Keller et al., 2008; Mort et al., 2008; Gertsch et al., 2010b). The magnitude of the OAE2 $\delta^{13}C$ excursion (~4.5‰) is comparable to the Wadi El Ghaib section in the eastern Sinai (5‰, Gertsch et al., 2010a), Eastbourne, England (~5‰, Jarvis et al., 2006), Tarfaya and Agadir, Morocco (3-4‰, Keller et al., 2008; Mort et al., 2008; Gertsch et al., 2010b), but higher than at Pueblo, Colorado (~2.5‰, Keller et al., 2004) and Azazoul, Morocco (~3‰, Gertsch et al., 2010b) (Fig. 11). This reveals that the OAE2 $\delta^{13}C$ excursion, which is mainly known from black shale deposits of deeper marine environments, reached into inner shelf and coastal environments, as earlier observed by Gertsch et al. (2010a, b) and confirmed in this study. However, the characteristic anoxic conditions of the $\delta^{13}C$ plateau are not apparent in the lithology of the studied sections (Figs. 3, 4).

8.2. Delayed OAE2 anoxia

Gertsch et al. (2010a, b) observed that in shallow near-shore environments anoxic conditions were not reached until the early Turonian and well after the OAE2

$\delta^{13}C$ plateau in the Wadi El Ghaib section of the Sinai and in northern Morocco (Azazoul section). This study confirms these observations in the Wadi Dakhl and Wadi Feiran sections. Lithologically, the delayed anoxic conditions are indicated by the presence of red laminated shales in the early Turonian of shallow C/T sections in Egypt and Morocco (Fig. 11). These red shales are diagentic products of the originally dark organic-rich shales (Voigt et al., 2006, 2007; Gertsch et al., 2010a, b). Neither planktic nor benthic foraminifera are observed in these red shales, which suggest anoxia comparable to the $\delta^{13}C$ plateau. The delay in anoxic conditions is considerable and probably encompasses most of ammonite zone T1. In all sections it occurs after the OAE2 $\delta^{13}C$ plateau in the early Turonian, although the timing appears to depend on local environmental conditions. The delayed anoxic conditions in inner shelf areas appears to be related to the sea level transgression, which reached its maximum in the early Turonian transporting low oxygen waters shoreward, which resulted in organic-rich shale deposition (see also Gertsch et al., 2010a, b). Despite this delay, the $\delta^{13}C$ excursion that characterizes OAE2 in marine environments is comparable and coeval to that in deeper open marine environments, including the stratotype at Pueblo, Colorado (Fig. 11).

9. Conclusions

- Biostratigraphic control in shallow water sequences is difficult due to low diversity and sporadic occurrences, though integrated macro- and microfossil biostratigraphy and stable isotope stratigraphy yields good age control for late Cenomanian to early Turonian sequences.
- Subtidal to inner neritic environments during the late Cenoamnian OAE2 excursion at Wadi Dakhl and Wadi Feiran are characterized by dysoxic, brackish

and mesotrophic conditions, as indicated by low species diversity, low oxygen and low salinity tolerant planktic and benthic species, along with oyster-rich limestone layers.

- The late Cenomanian OAE2 $\delta^{13}C$ excursion is recorded in shallow inner neritic environments of NE Egypt, and appears coeval with the OAE2 $\delta^{13}C$ excursion in open marine environments.
- Anoxic conditions characteristic of the late Cenomanian OAE2 are delayed until the early Turonian in shallow shelf sequences. This delay appears to be associated with the maximum sea level transgression in the early Turonian that transported low oxygen waters shoreward.

Acknowledgements

We thank the reviewers M. Hart, D. Horne and one anonymous, for comments and helpful suggestions. This study was supported through a grant from the Binational Fulbright Commission in Egypt to A. El-Sabbagh while visiting Princeton University, and partly supported by the U.S. National Science Foundation under Grant No. 0217921.

References

Abdel-Gawad, G., 1999. Biostratigraphy and facies of the Turonian in West Central Sinai, Egypt. Annals of the Geological Survey of Egypt 22, 99-114.

Abed, A.M., Sadaqah, R., 1998. Role of upper Cretaceous oyster bioherms in the deposition and accumulation of high-grade phosphorites in central Jordan. Journal of Sedimentary Research 68, 1009–1020.

Accarie, A., Emmanuel, L., Robaszynski, R., Baudin, F., Amedro, F., Caron, M., Deconinck, J., 1996. Carbon isotope geochemistry as stratigraphic tool. A case study of the Cenomanian/Turonian boundary in central Tunisia. Comptes Rendus de l'Académie des Sciences Paris (2a) 322, 579–586.

Amédro, F., Robaszynski, F., 2008. Zonation by ammonites and foraminifers of the Vraconian-Turonian interval: A comparison of the Boreal and Tethyan domains (NW Europe/Central Tunisia). Carnets de Géologie Letter 2 (CG2008-LO2), 1-5.

Arthur, M.A., Allard, D., Hinga, K.R., 1991. Cretaceous and Cenozoic atmospheric carbon dioxide variations and past global climate change. Abstract Program, Geological Society of America 23, 5178.

Arthur, M.A., Dean, W.E., Schlanger, S.O., 1985. Variations in the global carbon cycle during the Cretaceous related to climate, volcanism, and changes in atmospheric CO2. In: Sundquist, E.T., Broecker, W.S. (Eds.), The Carbon Cycle and Atmospheric CO2: Natural Variations Archean to Present, American Geophysical Union Monograph, vol. 32, pp. 504– 529.

Arthur, M.A., Jenkyns, H.C., Brumsack, H.J., Schlanger, S.O., 1990. Stratigraphy, geochemistry and paleoceanography of organic carbon-rich Cretaceous sequences. In: Ginsburg, R.N., Beaudoin, B. (Eds.), Cretaceous Resources, Events and Rhythms: Background and Plans for Research. NATO ASI series, pp. 75–119.

Arthur, M.A., Sageman, B.B., 1994. Marine black shales: depositional mechanisms and environments of ancient deposits. Annual Review of Earth and Planetary Sciences 22, 499–551.

Bachmann, M., Kuss, J., 1998. The middle Cretaceous carbonate ramp of the northern Sinai: sequence stratigraphy and facies distribution. In: Wright, V.P., Burchette, T.P. (Eds.), Carbonate ramps. Journal of the Geological Society, London, Special Publication 149, pp. 253-280.

Bandel, K., Kuss, J., Malchus, N., 1987. The sediments of Wadi Qena area, Eastern Desert, Egypt. Journal of African Earth Sciences 6, 427-455.

Bauer, J., Kuss, J., Steuber T., 2003. Sequence architecture and carbonate platform configuration (Late Cenomanian–Santonian), Sinai, Egypt. Sedimentology 50, 387–414.

Bauer, J., Marzouk, A.M., Steuber, T., Kuss, J., 2001. Lithostratigraphy and biostratigraphy of the Cenomanian-Santonian strata of Sinai, Egypt. Cretaceous Research 22, 497-526.

Birkelund, T., Hancock, J.M., Hart, M.B., Rawson, P.F., Remane, J., Robaszynski, F., Schmid, F., Surlyk, F., 1984. Cretaceous Stage boundaries, proposals. Bulletin of the Geological Society of Denmark 33, 3-20.

Bolli, H.M., Beckmann, J.-P., Sauders, J.B., 1994. Benthic foraminiferal biostratigraphy of the south Caribbean region. Cambridge University press, 408 pp.

Bralower, T.J., 1988. Calcareous nannofossil biostratigraphy and assemblages of the Cenomanian-Turonian boundary interval: implications for the origin and timing of oceanic anoxia. Palaeoceanography 3, 275-316.

Bralower, T.J., Leckie, R.M., Sliter, W.V., Thierstein, H.R., 1995. An integrated Cretaceous microfossil biostratigraphy. Society of Economic Paleontologists and Mineralogists Special Publication 54, 65-79.

Buchem, F.S.P., Van, Razin, P., Homewood, P.W., Heiko Oterdom, W., Philip J., 2002. Stratigraphic organization of carbonate ramps and organic-rich intraself: Natih

Formation (middle Cretaceous) of northern Oman. American Association of Petroleum Geologists 86, 21-53.

Bukry, D., 1973. Coccolith and silicoflagellate stratigraphy, Tasman Sea and southwestern Pacific Ocean, Deep Sea Drilling Project Leg 21. Initial Reports of the Deep Sea Drilling Project 21, 885-893.

Burnett, J.A., 1998. Upper Cretaceous. In: Bown, P.R. (Ed.), Calcareous nannofossil biostratigraphy. British Micropalaeontological Society Publication Series, Chapman and Hall Ltd. Kluwer Academic Publisher, London, pp. 132-165.

Canfield, D.E., 1994. Factors influencing organic carbon preservation in marine sediments. Chemical Geology 114, 315–329.

Caron, M., 1985. Cretaceous planktonic foraminifera. In: Bolli, H.M., Saunders, J.B., Perch-Nielsen, K. (Eds.), Plankton Stratigraphy. Cambridge University Press, Cambridge, pp. 17–86.

Caron, M., Dall'Agnolo, S., Accarie, H., Barrera, E., Kauffman, E.G., Amedro, F., Robaszynski, F., 2006. High-resolution stratigraphy of the Cenomanian-Turonian boundary interval at Pueblo (USA) and Wadi Bahloul (Tunisia): stable isotope and bio-events correlation. Geobios 39, 171–200.

Cepek, P., Hay, W.W., 1969. Calcareous nannoplankton and stratigraphic subdivision of the Upper Cretaceous. Transactions of the Gulf Coast Association of Geological Societies 19, 323-336.

Chancellor, G.R., Kennedy, W.J., Hancock, J.M., 1994. Turonian ammonite faunas from Central Tunisia. Journal of the Geological Society, London, Special Papers in Palaeontology 50, 1-118 p.

Cherif, O.H., Al-Rifaiy, I.A., Al-Afifi, F.I., Orabi, O.H., 1989. Foraminiferal biostratigraphy and paleoecology of some Cenomanian-Turonian exposures in West-Central Sinai (Egypt). Revue de Micropalèontologie 31, 243-262.

Cobban, W.A., Hook, S.C., 1980. The Upper Cretaceous (Turonian) ammonite Family Coilopoceratidae Hyatt in the western Interior of the United States. US Geological Survey Professional Paper 1192, 1-28.

Courtillot, V.E., Renne P.R., 2003. On the ages of flood basalt events. Comptes Rendus Geoscience 335, 113-140.

Cushman, J.A., 1946. Upper Cretaceous foraminifera of the Gulf Coast region of the United States and adjacent areas. US Geological Survey Professional Paper 206, 1-241.

Davey, S.D., Jenkyns, H.C., 1999. Carbon-isotope stratigraphy of shallow-water limestones and implications for the timing of Late Cretaceous sea-level rise and anoxic events (Cenomanian-Turonian of the peri-Adriatic carbonate platform, Croatia). Eclogae Geologicae Helvetiae 92, 163-170.

Dhondt, A.V., Malchus, N., Boumaza, L., Jaillard, E., 1999. Cretaceous oysters from North Africa: origin and distribution. Bulletin de la Société géologique de France 170, 67–76.

Drzewiecky, P.A., Simo, J.A., 1997. Carbonate platform frowning and oceanic anoxic events on a mid-Cretaceous carbonate platform, south-central Pyrenees, Spain. Journal of Sedimentary Research 67, 698-714.

El-Hedeny, M.M., 2002. Cenomanian-Coniacian ammonites from west-central Sinai, Egypt, and their significance in biostratigraphy. Neues Jahrbuch für Geologie und Paläontologie Monatshefte 7, 397-425.

El-Sabbagh, A.M., 2000. Stratigraphical and paleontological studies of the Upper Cretaceous succession in Gebel Nezzazat and Bir El-Markha areas, West-Central Sinai, Egypt. Unpublished PhD Thesis, Alexandria University, Faculty of Science, 209 pp.

El-Sabbagh, A.M., 2008. Shallow-water macrofaunal assemblages of the Cenomanian-Turonian sequence of Musabaa Salama area, west central Sinai, Egypt. Egyptian Journal of Paleontology 8, 63-86.

Erba, E., l987. Mid-Cretaceous cyclic pelagic facies from the Umbria-Marchean basin: what do calcareous nannofossils suggest? International Nannofossil Association Newsletter 9, 52-53.

Erba, E., Castradori, D., Guasti, G., Ripepe, M., 1992. Calcareous nannofossils and Milankovitch cycles: the example of the Albian Gault Clay Formation (southern England). Palaeogeography, Palaeoclimatology, Palaeoecology 93, 47–69.

Erba, E., Tremolada, F., 2004. Nannofossil carbonate fluxes during the early Cretaceous: phytoplankton response to nutrification episodes, atmospheric CO2, and anoxia. Paleoceanography 19, 1008. doi:10.1029/2003PA000884.

Erbacher, J., Hemleben, Ch., Huber, B.T., Markey, M., 1999. Correlating environmental changes during early Albian oceanic anoxic event 1B using benthic foraminiferal paleoecology. Marine Micropaleontology 38, 7-28.

Eshet, Y., Almogi Labin A., 1996. Calcareous nannofossils as paleoproductivity indicators in Upper Cretaceous organic-rich sequences in Israel. Marine Micropaleontology 29, 37-61.

Forster, A., Schouten, S., Baas, M., Sinninghe Damsté, J.S., 2007. Mid-Cretaceous (Albian-Santonian) sea surface temperature record of the tropical Atlantic Ocean. Geology 35, 919–922.

Gale, A.S., Smith, A.B., Monks, N.E.A., Young, J.A., Howard, A., Wray, D.S., Huggett, J.M., 2000. Marine biodiversity through the Late Cenomanian-Early Turonian: paleoceanographic controls and sequence stratigraphic biases. Journal of the Geological Society, London 157, 745-757.

Gebhardt, H. Friedrich, O. Schenk, B., Fox, L., Hart, M., Wagreich, M., 2010. Paleoceanographic changes at the northern Tethyan margin during the Cenomanian-Turonian Oceanic Anoxic Event (OAE2). Marine Micropaleontology 77, 25-45.

Gertsch, B., Adatte, T., Keller, G., Tantawy, A.A., Berner, Z., Mort, H.P., Fleitmann, D., 2010b. Middle and late Cenomanian oceanic anoxic events in shallow and deeper shelf environments of NW Morocco. Sedimentology 57, 1430-1462.

Gertsch, B., Keller, G., Adatte, T., Berner, Z., Kassab, A.S., Tantawy, A.A., El-Sabbagh, A.M., Stueben, D., 2010a. Cenomanian-Turonian transition in shallow water sequence of the Sinai, Egypt. International Journal of Earth Sciences (Geologische Rundschau) 99, 165–182.

Ghorab, M.A., 1961. Abnormal stratigraphic features in Ras Gharib oilfield. Third Arab Petroleum Congress, Alexandria, pp. 1-10.

Glenn, C.R., Arthur, M.A., 1990. Anatomy and origin of a Cretaceous phosphorite-green sand giant, Egypt. Sedimentology 37, 123-148.

Graciansky, P.C., de, Deroo, G., Herbin, J.P., Jacquin, T., Magni, F., Montadert, I., Müller, C., 1986. Ocean-wide stagnation episodes in the Late Cretaceous. Geological Rundschau 75, 17– 41.

Gustafsson, M., Holbourn, A., Kuhnt W., 2003. Changes in Northeast Atlantic temperature and carbon flux during the Cenomanian/Turonian

paleoceanographic event: the Goban Spur stable isotope record. Palaeogeography, Palaeoclimatology, Palaeoecology 201, 51-66.

Hallam, A., 1992. Phanerozoic Sea Level Changes. Columbia University Press, New York, 266 pp.

Haq, B.U., Hardenbol, J., Vail, P.R., 1987. Chronology of fluctuating sea levels since the Triassic. Science 235, 1156–1167.

Hardenbol, J., Caron, M., Amedro, F., Dupuis, Ch., Robaszynski, F., 1993. The Cenomanian-Turonian boundary in central Tunisia in the context of a sequence-stratigraphic interpretation. Cretaceous Research 14, 449-454.

Hardenbol, J., Thierry, J., Farley, M.B., de Graciansky, P.C., Vail, P.P., 1998. Mesozoic and Cenozoic sequence chronostratigraphic framework of European basins. Chart 4: Cretaceous sequence chronostratigraphy. In: de Graciansky, P.C., Hardenbol, J., Jacquin, T., Vail, P.P. (Eds.), Mesozoic and Cenozoic sequence stratigraphy of European basins, Society for Sedimentary Geology Special Publication 60, pp. 3-13.

Hart, M.B., 1980. A water depth model for the evolution of the planktonic foraminifera. Nature 286, 252–254.

Hart, M.B., 1999. The evolution and biodiversity of Cretaceous planktonic Foraminiferida. Geobios 32, 247–255.

Hart, M.B., Callapez, P.M., Fisher, J.K., Hannant, K., Monteiro, J.F., Price, G.D., Watkinson, M.P., 2008. Micropaleontology and stratigraphy of the Cenomanian/Turonian boundary in the Lusitanian Basin, Portugal. Journal of Iberian Geology 31, 311-326.

Hart, M.B., Dodsworth, P., Duane, A.M., 1993. The late Cenomanian Event in eastern England. Cretaceous Research 14, 495-508.

Hart, M.B., Leary, P.N., 1989. The stratigraphic and paleoceanographic setting of the late Cenomanian ‘‘anoxic’’ event. Journal of the Geological Society, London 146, 305–310.

Howe, R.W., Haig, D.W., Apthorpe, M.C., 2000. Cenomanian-Coniacian transition from siliciclastic to carbonate marine deposition, Giralia Anticline, Southern Carnarvon Platform, Western Australia. Cretaceous Research 21, 517–551

Huber, B.T., Norris, R.D., MacLeod, K.G., 2002. Deep-sea paleotemperature record of extreme warmth during the Cretaceous. Geology 30, 123-126.

Issawi, B., El Hinnawi, M., Francis, M., Mazhar, A., 1999. The Phanerozoic geology of Egypt: A geodynamic approach. Geological Survey of Egypt 76, 1-462.

Jarvis, I., Carson, G.A., Cooper, M.K.E., Hart, M.B., Leary, P.N., Tocher, B.A., Horne, D. and Rosenfeld, A., 1988. Microfossil assemblages and the Cenomanian/Turonian (Late Cretaceous) Oceanic Anoxic Event. Cretaceous Research 9, 3-103.

Jarvis, I., Gale, A.S., Jenkyns, H.C., Pearce, M.A., 2006. Secular variation in Late Cretaceous carbono isotopes: a new $\delta^{13}C$ carbonate reference curve for the Cenomanian-Campanian (99.6-70.6 Ma). Geological Magazine 143, 561-608.

Jenkyns, H.C., Gale, A.S., Corfield, R.M., 1994. Carbon- and oxygen-isotope stratigraphy of the English Chalk and Italian Scaglia and its palaeoclimatic significance. Geological Magazine 131, 1–34.

Kassab, A.S., 1991. Cenomanian-Coniacian biostratigraphy of the northern Eastern Desert, Egypt, based on ammonites. Newsletters on Stratigraphy 25, 25–35.

Kassab, A.S., 1994. Upper Cretaceous ammonites from the El-Sheikh Fadl-Ras Gharib Road, Northeastern Desert, Egypt. Neues Jahrbuch für Geologie und Paläontologie Monatshefte 2, 108-128.

Kassab, A.S., 1999. Cenomanian–Turonian boundary in the Gulf of Suez region, Egypt: towards an inter-regional correlation, based on ammonites. Geological Society of Egypt, Special Publication 2, 61–98.

Kassab, A.S., Ismael, M.M., 1994. Upper Cretaceous invertebrate fossils from the area northeast of Abu Zeneima, Sinai, Egypt. Neues Jahrbuch für Geologie und Paläontologie Abhandlungen 191, 221–249

Kassab, A.S., Obaidalla, N.A., 2001. Integrated biostratigraphy and interregional correlation of the Cenomanian–Turonian deposits of Wadi Feiran, Sinai, Egypt. Cretaceous Research 22, 105–114.

Keller, G., Abramovich, S., 2009. Lilliput effect in late Maastrichtian planktic foraminifera: Response to environmental stress. Palaeogeography, Palaeoclimatology, Palaeoecology 284, 47-62.

Keller, G., Adatte, T., Berner, Z., Chellai, E.H., Stueben, D., 2008. Oceanic events and biotic effects of the Cenomanian-Turonian anoxic event, Tarfaya Basin, Morocco. Cretaceous Research 29, 976-994.

Keller, G., Berner, Z., Adatte, T., Stueben, D., 2004. Cenomanian-Turonian $\delta^{13}C$ and $\delta^{18}O$, sea level and salinity variations at Pueblo, Colorado. Palaeogeography, Palaeoclimatology, Palaeoecology 211, 19–43.

Keller, G., Han, Q., Adatte, T., Burns, S., 2001. Paleoenvironment of the Cenomanian-Turonian transition at Eastbourne, England. Cretaceous Research 22, 391–422.

Keller, G., Li, L., MacLeod, N., 1995. The Cretaceous/Tertiary boundary stratotype section at El Kef, Tunisia: how catastrophic was the mass extinction? Palaeogeography, Palaeoclimatology, Palaeoecology 119, 221-254.

Keller, G., Pardo, A., 2004. Age and paleoenvironment of the Cenomanian-Turonian global stratotype section and point at Pueblo, Colorado. Marine Micropaleontology 51, 95–128.

Kennedy, W.J., Cobban, W.A., 1991. Stratigraphy and interregional correlation of the Cenomanian-Turonian transition in the Western Interior of the United States near Pueblo, Colorado, a potential boundary stratotype for the base of the Turonian stage. Newsletters on Stratigraphy 24, 1–33.

Kennedy, W.J., Walaszezyk, I., Cobban, W.A., 2000. Pueblo, Colorado, USA, candidate Global Boundary Stratotype Section and Point for the base of the Turonian Stage of the Cretaceous and for the base of the middle Turonian Substage, with a revision of the Inoceramidae (Bivalvia). Acta Geologica Polonica 50, 295–334.

Kennedy, W.J., Wright, C.W., Hancock, J.M., 1987. Basal Turonian ammonites from West Texas. Palaeontology 30, 27–74.

Kerdany, M.T., Cherif, O.H., 1990. Mesozoic. In: Said, R. (Ed.), The geology of Egypt. Balkema Publishers, pp. 407-438.

Kolonic, S., Sinninghe Damsté, J.S., Bottcher, M.E., Kuypers, M.M.M., Kuhnt, W., Beckmann, B., Scheeder, G., Wagner, T., 2002. Geochemical characterization of Cenomanian/Turonian black shales from the Tarfaya Basin (SW Morocco) – relationships between palaeoenvironmental conditions and early sulphurization of sedimentary organic matter. Journal of Petroleum Geology 25, 325–350.

Kolonic, S., Wagner, T., Forster, A., Sinningh Damsté , J.S., Walsworth-Bell, B., Erba, E., Turgeon, S., Brumsack, H.J., Chellai, E.H., Tsikos, H., Kuhnt, W., Kuypers, M.M.M., 2005. Black shale deposition on the northwest African shelf during the

Cenomanian-Turonian oceanic anoxic event: climate coupling and global organic carbon burial. Paleoceanography 20, 1006. doi:10.1029/2003PA000950.

Kora, M., Hamama, H.H., 1987. Biostratigraphy of the Cenomanian-Turonian successions of Gebel Gunna, southeastern Sinai, Egypt. Mansoura Faculty of Science Bulletin 14, 289–301.

Kora, M., Khalil, H., Sobhy, M., 2001. Stratigraphy and microfacies of some Cenomanian-Turonian successions in the Gulf of Suez Region. Egyptian Journal of Geology 45, 413-439.

Kora, M., Shahin, A., Semiet, A., 1994. Biostratigraphy and paleoecology of some Cenomanian successions in the West-Central Sinai, Egypt. Neues Jahrbuch für Geologie und Paläontologie Monatshefte 10, 597-617.

Koutsoukos, E.A.M., Leary, P.N., Hart, M.B., 1990. Latest Cenomanian-earliest Turonian low-oxygen tolerant benthonic foraminifera: a case study from the Sergipe Basin (N.E. Brazil) and the western Anglo-Paris Basin (Southern England). Palaeogeography, Palaeoclimatology, Palaeoecology 77, 145–177.

Kuhnt, W., Luderer, F., Nederbragt, S., Thurow, J., Wagner, T., 2005. Orbital scale record of the late Cenomanian-Turonian Oceanic Anoxic Event (OAE2) in the Tarfaya Basin (Morocco). International Journal of Earth Sciences 94, 147–159.

Kuhnt, W., Nederbragt, A., Leine, L., 1997. Cyclicity of Cenomanian-Turonian organic-carbon-rich sediments in the Tarfaya Atlantic Coastal Basin (Morocco). Cretaceous Research 18, 587-601.

Kuss, J., 1992. Facies and stratigraphy of Cretaceous limestones from northeast Egypt, Sinai, and southern Jordan. Geology of the Arab World, Cairo University, 283-302.

Kuss, J., Bachmann, M., 1996. Cretaceous paleogeography of the Sinai Peninsula and

neighboring areas. Comptes rendus de l'Academie des Sciences, Serie II, Sciences de la Terre et des Planetes 322, 915-933.

Lamolda, M.A., Gorostidi, A., Paul, C.R.C., 1994. Quantitative estimates of calcareous nannofossil changes across the Plenus Marls (latest Cenomanian), Dover, England; implication for the generation of the Cenomanian-Turonian boundary event. Cretaceous Research 15, 143-164.

Leckie, R.M., 1987. Paleoecology of the mid-Cretaceous planktic foraminifera: a comparison of open ocean and epicontinental sea assemblages. Micropaleontology 33, 164–176.

Leckie, R.M., Bralower, T.J., Cashman, R., 2002. Oceanic anoxic events and plankton evolution: biotic response to tectonic forcing during the mid-Cretaceous. Paleoceanography 17, 1041. doi:10.1029/2001PA000623.

Leckie, R.M., Yuretich, R.F., West, L.O.L., Finkelstein, D., Schmidt, M., 1998. Paleoceanography of the southwestern Western Interior Sea during the time of the Cenomanian-Turonian boundary (Late Cretaceous). In: Dean, W.E., Arthur, M.A. (Eds.), Concepts in Sedimentology and Paleontology. Society of Economic Paleontologists and Mineralogists 6, pp. 101–126.

Lees, J., 2002. Calcareous nannofossil biogeography illustrates palaeoclimate change in the Late Cretaceous Indian Ocean. Cretaceous Research 23, 537-634.

Lewy, Z., Kennedy, J. and Chancellor, G., 1984. Co-occurrence of *Metoicoceras geslinianum* (d'Orbigny) and *Vascoceras cauvini* Chudeau (Cretaceous Ammonoidea) in the southern Negev (Israel) and its stratigraphic implications. Newsletters on Stratigraphy 13, 67-76.

Lewy, Z., Raab, M., 1976. Mid-Cretaceous stratigraphy of the Middle East. Annals du Muséum d'Histoire Naturelle de Nice 4 (XXXII), 1-17.

Linnert, C., Mutterlose, J., Erbacher, J., 2010. Calcareous nannofossils of the Cenomanian/Turonian boundary interval from the Boreal Realm (Wunstorf, northwest Germany). Marine Micropaleontology 74, 38–58.

Luciani, V., Cobianchi, M., l999. The Bonarelli level and other black shales in the Cenomanian-Turonian of the northeastern Dolomites (Italy): calcareous nannofossil and foraminiferal data. Cretaceous Research 20, 135-167.

Lüning, S., Kolonic, S., Belhadj, E.M., Cota, L., Baric, G., Wagner, T., 2004. Integrated depositional model for the Cenomanian-Turonian organic-rich strata in North Africa. Earth-Science Reviews 64, 51-117.

Lüning, S., Marzouk, A., Morsi, A., Kuss, J., 1998. Sequence stratigraphy of the Upper Cretaceous of central-east Sinai, Egypt. Cretaceous Research 19,153–196.

Malchus, N., 1990. Revision der Kreide-Austern (Bivalvia: Pteriomorphia) Ägyptens (Biostratigraphie, Systematik). Berliner Geowissenschäftliche Abhandlungen A125, 1-231.

Manivit, H., Perch-Nielsen, K., Prins, B., Verbeek, J.W., 1977. Mid Cretaceous calcareous nannofossil biostratigraphy. Proceedings of the Koninklijke Nederlandse Akademie van Wetenschappen, Series B80, 169-181.

Marshall, J.D., 1992. Climatic and oceanographic isotopic signals from the carbonate rock record and their preservation. Geological Magazine 129, 143-160.

Meister, C., Abdallah, H., 2005. Précision sur les successions d'ammonites du Cénomanien-Turonien dans la région de Gafsa, Tunisie du centre-sud. Revue de Paléobiologie 24, 111-199.

Meister, C., Allzuma, K., Mathey, B., 1992. Les ammonites du Niger (Afrique occidentale) et la Transgression Transsaharienne au cours du Cenomanien–Turonien. Geobios 25, 55–100

Meister, C., Rhalmi, M., 2002. Quelques ammonites du CénomanieneTuronien de la région d'Errachidia-Boudnid-Erfoud (partie méridionale du Haut Atlas Central, Maroc). Revue de Paléobiologie 21, 759-779.

Mitchell, S.F., Ball, J.D., Crowley, S.F., Marshall, J.D., Paul, C.R.C., Veltkamp, C.J., Samir, A., 1997. Isotope data from Cretaceous chalks and foraminiferal environmental or diagenetic signals? Geology 25, 691–694.

Mort, H., Adatte, T., Keller, G., Bartels, D., Föllmi, K., Steinmann, P., Berner, Z., Chellai, E.H., 2008. Organic carbon deposition and phosphorus accumulation during Oceanic Anoxic Event 2 in Tarfaya, Morocco. Cretaceous Research 29, 1008-1023.

Murray, J.W., 1973. Deposition and ecology of living benthic foraminiferids. Russak and Co, Carne, pp 1–274.

Mutterlose, J., 1989. Temperature-controlled migration of calcareous nannofossils in the north-west European Aptian. In: Crux, J.A., van Heck, S.E. (Eds.), Nannofossils and their applications. Chichester (Ellis Horwood), pp. 122–142.

Mutterlose, J., Bornemann, A., Herrle, O., 2005. Mesozoic calcareous nannofossils – state of the art. Paläontologische Zeitschrift 79, 113–133.

Mutterlose, J., Kessels, K., 2000. Early Cretaceous calcareous nannofossils from high latitudes: implications for palaeobiogeography and palaeoclimate. Palaeogeography, Palaeoclimatology, Palaeoecology 160, 347–372.

Mutterlose, J., Luppold, F.W., Grenda, F., 1994. Floren- und Faunenverteilung in rhythmisch gebankten Serien des Hauterive (Unterkreide) NW Deutschlands. Berichte der Naturhistorischen Gesellschaft Hannover 136, 27–65.

Nagm, E., Wilmsen, M., Aly, M., Hewaidy, A., 2010a. Upper Cenomanian - Turonian (Upper Cretaceous) ammonoids from the western Wadi Araba, Eastern Desert, Egypt. Cretaceous Research 31, 473-499.

Nagm, E., Wilmsen, M., Aly, M., Hewaidy, A., 2010b. Biostratigraphy of the Upper Cenomanian - Turonian (lower Upper Cretaceous) successions of the western Wadi Araba, Eastern Desert, Egypt. Newsletters on Stratigraphy 44, 17-35.

Nederbragt, A.J., 1991. Late Cretaceous biostratigraphy and development of Heterohelicidae (planktic foraminifera). Micropaleontology 37, 329-372.

Nederbragt, A.J., 1998. Quantitative biogeography of late Maastrichtian planktic foraminifera. Micropaleontology 44, 385-412.

Nederbragt, A., Fiorentino, A., 1999. Stratigraphy and paleoceanography of the Cenomanian-Turonian boundary event in Oued Mellegue, northwestern Tunisia. Cretaceous Research 20, 47–62.

Norris, R.D., Bice, K.L., Magno, E.A., Wilson, P., 2002. Jiggling the tropical thermostat in the Cretaceous hothouse. Geology 30, 299–302.

Omara, S., 1956. New foraminifera from Cenomanian of Sinai, Egypt. Journal of Paleontology 30, 883-890.

Pardo, A., Keller, G., 2008. Biotic effects of environmental catastrophes at the end of the Cretaceous and early Tertiary: *Guembelitria* and *Heterohelix* blooms. Cretaceous Research 29, 1058–1073.

Parente, M., Frijia, G., Di Lucia, M., 2007. Carbon-isotope stratigraphy of Cenomanian-Turonian platform carbonates from the southern Apennines (Italy): a chemostratigraphy approach to the problem of correlation between shallow-water and deep-water successions. Journal of the Geological Society, London 164, 609-620.

Paul, C.R.C., Lamolda, M.A., Mitchell, S.F., Vaziri, M.R., Gorostidi, A., Marshall, J.D., 1999. The Cenomanian-Turonian boundary at Eastbourne (Sussex, UK): a proposed European reference section. Palaeogeography, Palaeoclimatology, Palaeoecology 150, 83–121.

Pedersen, T.F., Calvert, S.E., 1990. Anoxia vs. Productivity: what controls the formation of organic-carbon-rich sediments and sedimentary rocks? American Association of Petroleum Geologists 74, 454-466.

Perch-Nielsen, K., 1979. Calcareous nannofossils from the Cretaceous between the North Sea and the Mediterranean. Aspekte der Kreide Europas. International Union of Geological Sciences Series A6, 223–272.

Perch-Nielsen, K., 1985. Cennozoic calcareous nannofossils. In: Bolli, H.M., Saunders, J.B., Perch-Nielsen, K. (Eds.), Plankton Stratigraphy. Cambridge University Press, Cambridge, pp. 422-454.

Perty D., Lamolda, M., 1996. Benthonic foraminiferal mass extinction and survival assemblages from the Cenomanian–Turonian boundary event in the Menoyo section, northern Spain. In: Hart, M. (Ed.), Biotic recovery from mass extinction events. Journal of the Geological Society, London, Special Publication 102, pp. 245–258.

Philip, J., 2003. Peri-Tethyan neritic carbonate areas: distribution through time and driving factors. Palaeogeography, Palaeoclimatology, Palaeoecology 196, 19–37.

Premoli Silva, I., Erba, E., Salvini, G., Verga, D., Locatelli, C., 1999. Biotic changes in Cretaceous anoxic events. The Journal of Foraminiferal Research 29, 352-370.

Premoli Silva I., Sliter W.V., 1999. Cretaceous paleoceanography: evidence from planktonic foraminiferal evolution. In: Barrera E., Johnson C.C. (Eds.),

Evolution of the Cretaceous ocean-climate system. Geological Society of America, Special Paper 332, pp. 301-328.

Pucéat, E., 2008. A new breath of life for anoxia. Geology 36, 831-832.

Pucéat, E., Lécuyer, C., Donnadieu, Y., Naveau, P., Cappetta, H., Ramstein, G., Huber, B.T., Kriwet, J., 2007. Fish tooth $\delta^{18}O$ revising Late Cretaceous meridional upper ocean water temperature gradients. Geology 35, 107–110.

Pufahl, P.K., James, N.P., 2006. Monospecific Pliocene oyster buildups, Murray Basin, South Australia: Brackish water end member of the reef spectrum. Palaeogeography, Palaeoclimatology, Palaeoecology 233, 11-33.

Robaszynski, F., Caron, M., 1979. Atlas de foraminifères planctoniques du Crètacè moyen (Mer Boreale et Tethys), première partie. Cahiers de Micropalèontologie 1, 1-185.

Robaszynski, F., Caron, M., 1995. Foraminifères planctoniques du Crétacé: Commentaire de la zonation Europe-Méditerranée. Bulletin de la Société géologique de France 166 (6), 681-692.

Robaszynski, F., Caron, M., Dupuis, C., Amédro, F., Gonzalez Donoso, J. M., Linares, D., Hardenbol, J., Gartner, S., Calandra, F., Deloffre, R., 1990. A tentative integrated stratigraphy in the Turonian of central Tunisia: formations, zones and sequential stratigraphy in the Kalaat Senan area. Bulletin des Centres de Recherches Exploration-Production Elf Aquitaine 14, 213-384.

Robaszynski, F., Gale, A.S., 1993. The Cenomanian–Turonian boundary: a discussion held at the final session of the colloquium on the Cenomanian–Turonian events, Grenoble, 26th May 1991 (France). Cretaceous Research 14, 607–611.

Roth, P.H., 1978. Cretaceous nannoplankton biostratigraphy and oceanography of the northwestern Atlantic Ocean. In: Benson, W.E., Sheridan, R.E. (Eds.), Initial

Reports of the Deep Sea Drilling Project 44. U.S. Government Printing Office, Washington, DC, pp. 731–759.

Roth, P.H., 1981. Mid-Cretaceous calcareous nannoplankton from the Central Pacific: Implication for paleoceanography. Initial Report of the Deep Sea Drilling Project 62, 471-489.

Roth, P.H., Bowdler, J.L., 1981. Middle Cretaceous calcareous nannoplankton biostratigraphy and oceanography of the Atlantic Ocean. Society of Economic Paleontologists and Mineralogists Special Publication 32, 517-546.

Roth, P.H., Krumbach, K.R., 1986. Middle Cretaceous calcareous nannofossil biogeography and preservation in the Atlantic and Indian oceans: implications for palaeoceanography. Marine Micropaleontology 10, 235-266.

Sageman, B.B., Rich, J., Arthur, M.A., Dean, W.E., Savrda, C.E., Bralower, T.J., 1998. Multiple Milankovictch cycles in the Bridge Creek Limestone (Cenomanian-Turonian), Western Interior Basin. In: Dean, W.E., Arthur, M.A. (Eds.), Stratigraphy and Paleoenvironments of the Cretaceous Western Interior Seaway, USA. SEPM Concepts in Sedimentology and Paleontology 6, pp. 153-171.

Said, R., 1962. The Geology of Egypt. Elsevier, Amsterdam, 377 pp.

Said, R., 1990. The Geology of Egypt. Balkema Publishers, 734 pp.

Schrag, D.P., DePaolo, D.J., Richter, F.M., 1995. Reconstructing past sea surface temperatures: correcting for diagenesis of bulk marine carbon. Geochimica et Cosmochimica Acta 59, 2265–2278.

Schulze, F., Marzouk, A.M., Bassiouni, M.A., Kuss, J., 2004. The late Albian-Turonian carbonate platform succession of west-central Jordan: stratigraphy and crises. Cretaceous Research 25, 709-737.

Seton, M., Gaina, C., Müller, R.D., Heine, C., 2009. Mid-Cretaceous seafloor spreading pulse: Fact or fiction? Geology 37, 687-690.

Shafik, S., 1990. Late Cretaceous nannofossil biostratigraphy and biogeography of the Australian western margin. Bureau of Mineral Resources, Geology and Geophysics, Report 295, 1-164.

Shahin, A., Kora, M., 1991. Biostratigraphy of some Upper Cretaceous successions in the eastern Central Sinai, Egypt. Neues Jahrbuch für Geologie und Paläontologie Monatshefte 11, 671-692.

Sinton, C.W., Duncan, R.A., Storey, M., Lewis, J., Estrada, J.J., 1998. An oceanic flood basalt province within the Caribbean Plate. Earth and Planetary Science letters 155, 221– 235.

Sissingh, W., 1977. Biostratigraphy of Cretaceous calcareous nannoplankton. Geologie en Mijnbouw 56, 37-65.

Sliter, W.V., 1968. Upper Cretaceous foraminifera from southern California and northwestern Baja California, Mexico. University of Kansas Paleontological Contributions 49, 1-141.

Snow, L.J., Duncan, R.A., Bralower, T.J., 2005. Trace element abundances in the Rock Canyon Anticline, Pueblo, Colorado, marine sedimentary section and their relationship to Caribbean plateau construction and oxygen anoxic event 2. Paleoceangraphy, 20, PA3005. doi:10.1029/2004PA001093.

Tantawy, A.A., 2008. Calcareous nannofossil biostratigraphy and paleoecology of the Cenomanian-Turonian transition in the Tarfaya Basin, southern Morocco. Cretaceous Research 29, 996-1007.

Thierstein, H.R., 1980. Selective dissolution of late Cretaceous and earliest Tertiary calcareous nannofossils: Experimental evidence. Cretaceous Research 2, 165-

176.

Thierstein, H.R., 1981. Late Cretaceous nannoplankton and the change at the Cretaceous-Tertiary boundary. Society of Economic Paleontologists and Mineralogists Special Publication 32, 355-394.

Turgeon, S.C., Creaser, R.A., 2008. Cretaceous oceanic anoxic event 2 triggered by a massive magmatic episode. Nature 454, 323-326.

Voigt, S., Aurag, A., Leis, F., Kaplan, U., 2007. Late Cenomanian to middle Turonian high-resolution carbon isotope stratigraphy: New data from the Münsterland Cretaceous Basin, Germany. Earth and Planetary Science Letters 253, 196-210.

Voigt, S., Erbacher, J., Mutterlose, J., Weiss, W., Westerhold, T., Wiese, F., Wilmsen, M., Wonik, T., 2008. The Cenomanian – Turonian of the Wunstorf section – (North Germany): global stratigraphic reference section and new orbital time scale for Oceanic Anoxic Event 2. Newsletters on Stratigraphy 43, 65-89.

Voigt, S., Gale, A.S., Voigt, T., 2006. Sea-level change, carbon cycling and palaeoclimate during the Late Cenomanian of northwest Europe; an integrated palaeoenvironmental analysis. Cretaceous Research 27, 836-858.

Watkins, D.K., Wise, S.W., Pospichal, J.J., Crux, J., 1996. Upper Cretaceous calcareous nannofossil biostratigraphy and paleoceanography of the Southern Ocean. In: Moguilevsky, A., Whatley, R. (Eds.), Microfossils and oceanic environments. University of Wales, Aberystwyth Press, Aberystwyth, pp. 355–381.

Wilmsen, M., Nagm, E., 2009, Biofacies, stratigraphy and facies development of the Galala and Maghra El Hadida formations (Cenomanian-Turonian, Wadi Araba, Eastern Desert, Egypt). 8th International Symposium on the Cretaceous System, Abstract Volume, pp. 153-154.

Wright, C.W., Kennedy, W.J., Hancock, J.M., 1984. Introduction. In: Wright, C.W., Kennedy, W.J. (Eds.), The Ammonoidea of the Lower Chalk: Part I. Monograph of the Palaeontographical Society, London 1, pp. 1–37.

Zakhera, M., Kassab, A.S., 2002. Integrated macrobiostratigraphy of the Cenomanian-Turonian transition, Wadi El-Siq, west central Sinai, Egypt. Egyptian Journal of Paleontology 2, 219-233.

Figure and table captions

Fig. 1. Location map showing the sections analyzed across the Gulf of Suez and the Wadi El Ghaib section of Gertsch et al. (2010a) in the eastern Sinai.

Fig. 2. A, Geographic distribution of the Cenomanian-Turonian (C-T) organic-rich deposits in the Atlantic and adjacent areas (modified after De Graciansky et al., 1986). Stars mark the locations of studied sections (Egypt) and other C-T sections in Morocco and the U.S. Western Interior Basin. B, Late Cenomanian palaeogeographic map of the Peri-Tethyan domain with main depositional environments (modified after Philip, 2003). Square marks the study area of Figure 1.

Fig. 3. Lithological descriptions of the Wadi Dakhl section and photos of the outcrop showing part of the lower marl interval and the Cenomanian-Turonian transition.

Fig. 4. Lithological descriptions of the Wadi Feiran section and photo of the outcrop showing different rock facies, sample positions and the Cenomanian-Turonian boundary.

Fig. 5. $\delta^{13}C$ curves of the (A) Wadi Feiran and (B) Wadi Dakhl sections. $\delta^{13}C$ record at the Wadi Feiran section shows the characteristic positive excursion of the late Cenomanian OAE2. At Wadi Dakhl the $\delta^{13}C$ curve shows only a small part of the OAE2 plateau.

Fig. 6: Some selected late Cenomanian - late Turonian ammonite index species from the Wadi Dakhl section. A-B, *Neolobites vibrayeanus* (d'Orbigny, 1841), Upper

Cenomanian Raha Formation. A: ventral view, B: lateral view; scale bars = 1cm. C-D, *Vascoceras cauvini* Chudeau, 1909, Upper Cenomanian Abu Qada Formation. C: lateral view, D: ventral view; scale bar = 2 cm. E-G, *Vascoceras proprium* (Reyment, 1954), Lower Turonian Abu Qada Formation. E: apertural view, F: lateral view, G: ventral view; scale bars = 1.5 cm. H-I, *Choffaticeras segne* (Solger, 1903), Lower Turonian Abu Qada Formation. H: lateral view, scale bar = 1.5 cm; I: lateral view. J-K, *Coilopoceras requienianum* (d'Orbigny, 1841), Upper Turonian Wata Formation. J: apertural view, K: lateral view; scale bars = 2 cm.

Fig. 7. Late Cenomanian-late Turonian biostratigraphy of ammonites, oysters and planktic foraminifera with the benthic/planktic ratio and the $\delta^{13}C$ record of the Wadi Dakhl section. Biostratigraphic interpretation is based on fauna, the $\delta^{13}C$ curve and local and regional correlations.

Fig. 8. Late Cenomanian-early Turonian biostratigraphy of ammonite, nannoplankton and planktic and benthic foraminifera with the benthic/planktic ratio and the $\delta^{13}C$ record of the Wadi Feiran section. Biostratigraphic interpretation is based on fauna, flora, the $\delta^{13}C$ curve and local and regional correlations.

Fig. 9. Light microscope photographs of some selected calcareous nannofossil species from the Wadi Feiran section. All figures were taken under cross-polarized light. 1, *Axopodorhabdus albianus*, sample 14. 2, *Tranolithus phacelosus*, sample 5. 3, *Zeugrhabdotus scutula*, sample 22. 4, *Zeugrhabdotus erectus*, sample 10. 5, *Zeugrhabdotus embergeri*, sample 33. 6, *Helicolithus trabeculatus*, sample 14. 7, *Eiffellithus turriseiffelii*, sample 19. 8, *Rhagodiscus achlyostaurion*, sample 20. 9,

Rhagodiscus splendens, sample 19. 10, *Biscutum constans*, sample 38. 11, *Watznaueria barnesae*, sample 5. 12, *Retecapsa crenulata*, sample 38. 13, *Helenea chiastia*, sample 24. 14, *Prediscosphaera cretacea*, sample 17. 15, *Flabellites oblonga*, sample 33. 16, *Gartnerago obliquum*, sample 38. 17, *Broinsonia matalosa*, sample 38. 18, *Lithraphidites carniolensis*, sample 22. 19, *Microrhabdulus decoratus*, sample 38. 20, *Eprolithus octopetalus*, sample 28. 21-22, *Eprolithus floralis*, sample 26. 23, *Radiolithus planus*, sample 27. 24, *Quadrum gartneri*, sample 47.

Fig. 10. Cenomanian-late Turonian benthic foraminifera of the Wadi Dakhl section. Note that most benthic foraminiferal assemblages are diversified, sporadic and dominated mainly by agglutinated species.

Fig. 11. $\delta^{13}C$ correlation of the late Cenomanian OAE2 excursion in Egypt, Morocco and Pueblo. Note that the OAE2 $\delta^{13}C$ excursion is comparable in all sections. The absence of the characteristic two $\delta^{13}C$ peaks at the Wadi Dakhl section indicates a major hiatus. Dark grey areas mark OAE2, whereas light grey marks the interval between peaks 1 and 2. No anoxic conditions are observed during OAE2 in these shallow environments, but delayed anoxic conditions are observed in the early Turonian in Egypt and Morocco (darker grey areas). These delayed anoxic/dysoxic conditions are correlated with the maximum sea level transgression in shallow environments.

Table 1**.** Inter-regional correlation of the late Cenomanian-early Turonian ammonite zones for the Wadi Dakhl section.

Table 2. Comparison between commonly used calcareous nannofossil zonal schemes.

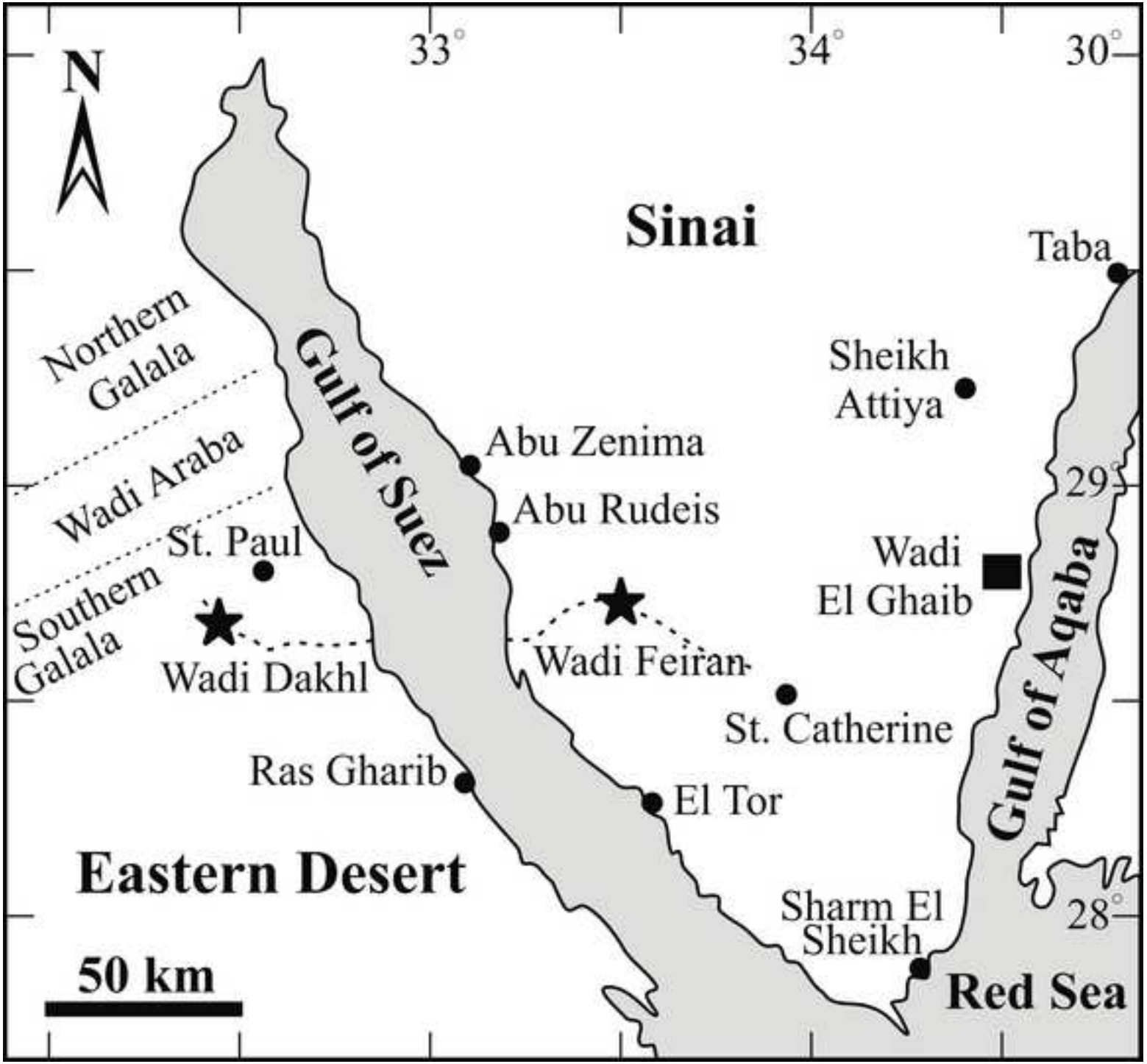

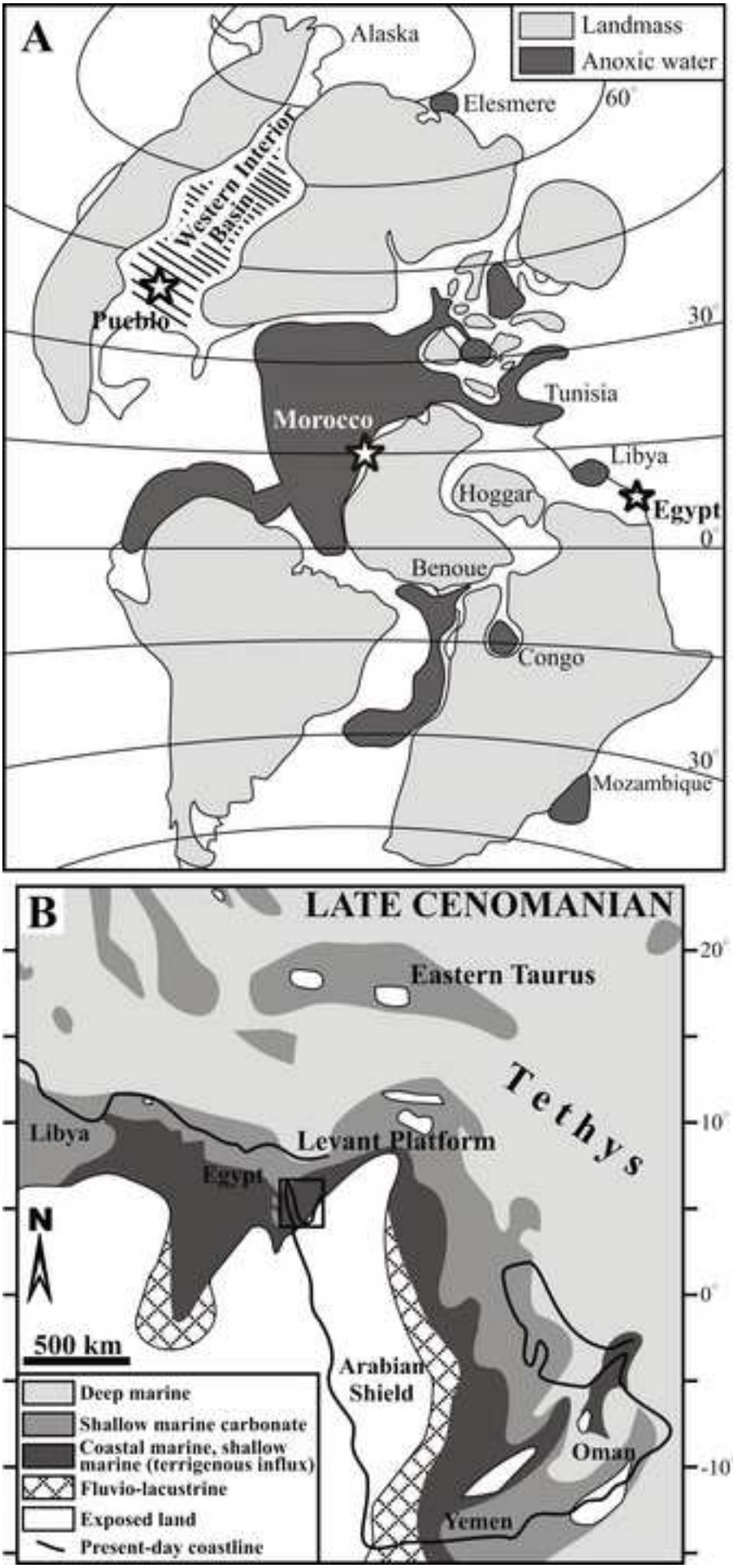

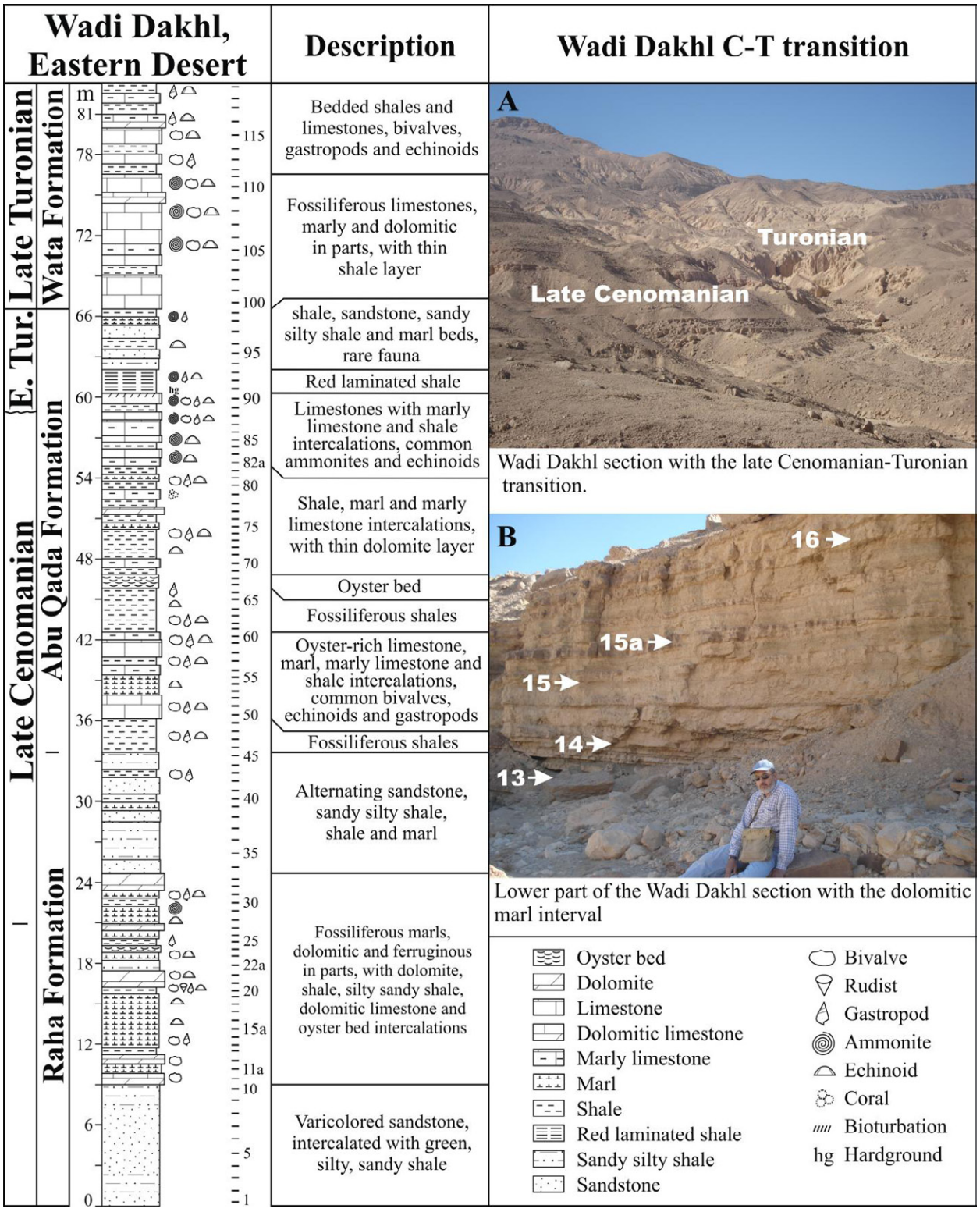

Figure 3

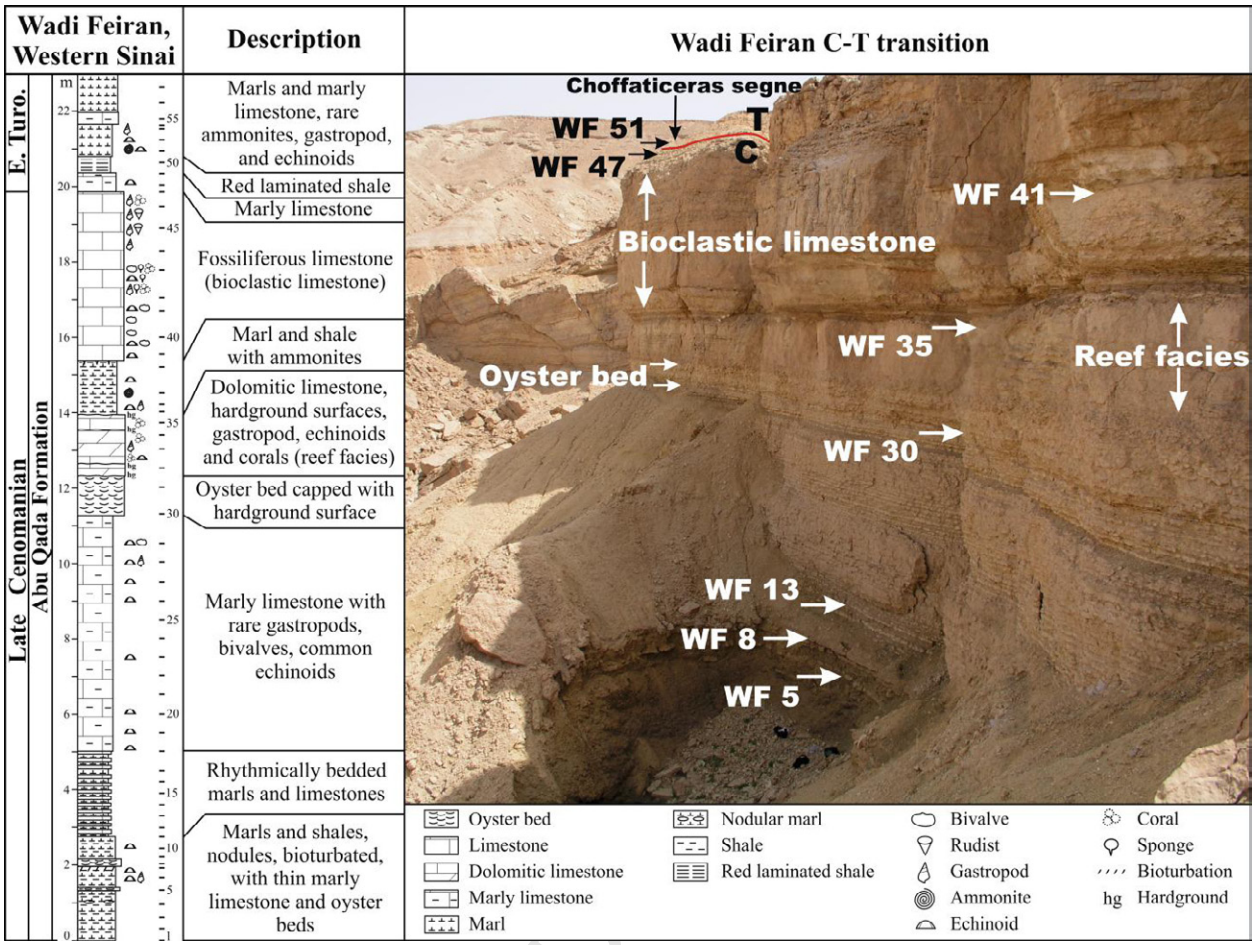

Figure 4

Figure

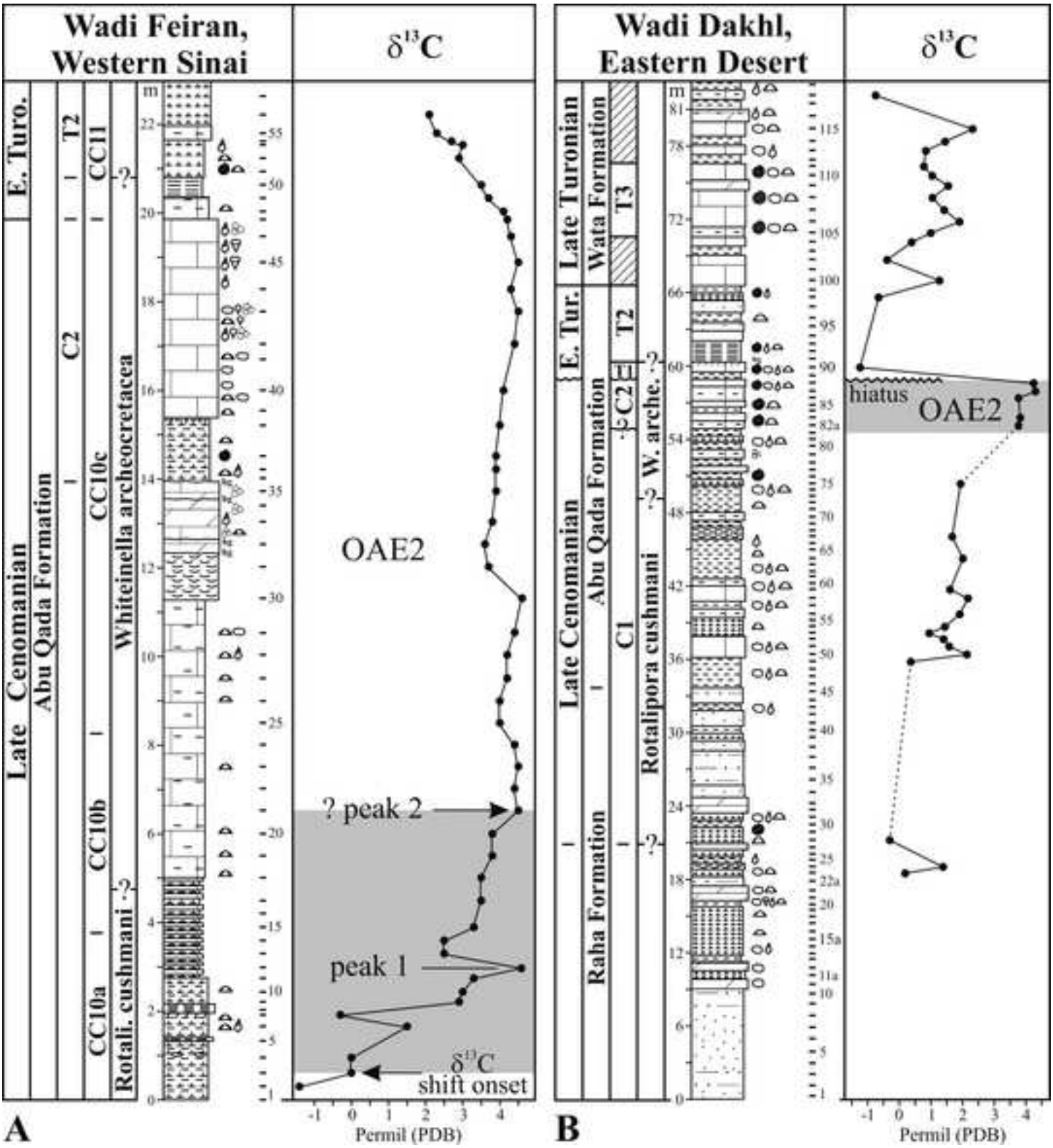

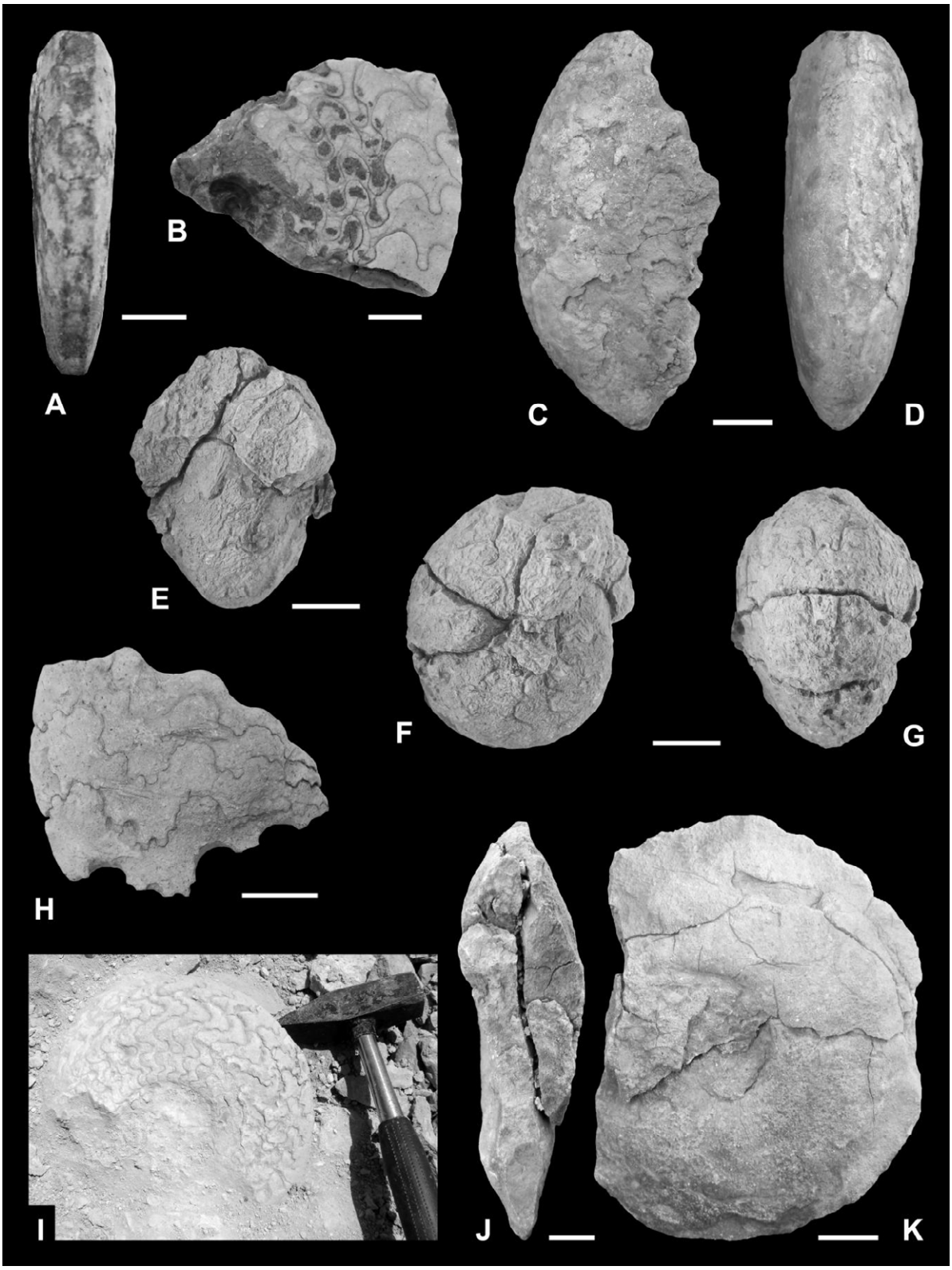

Figure 6

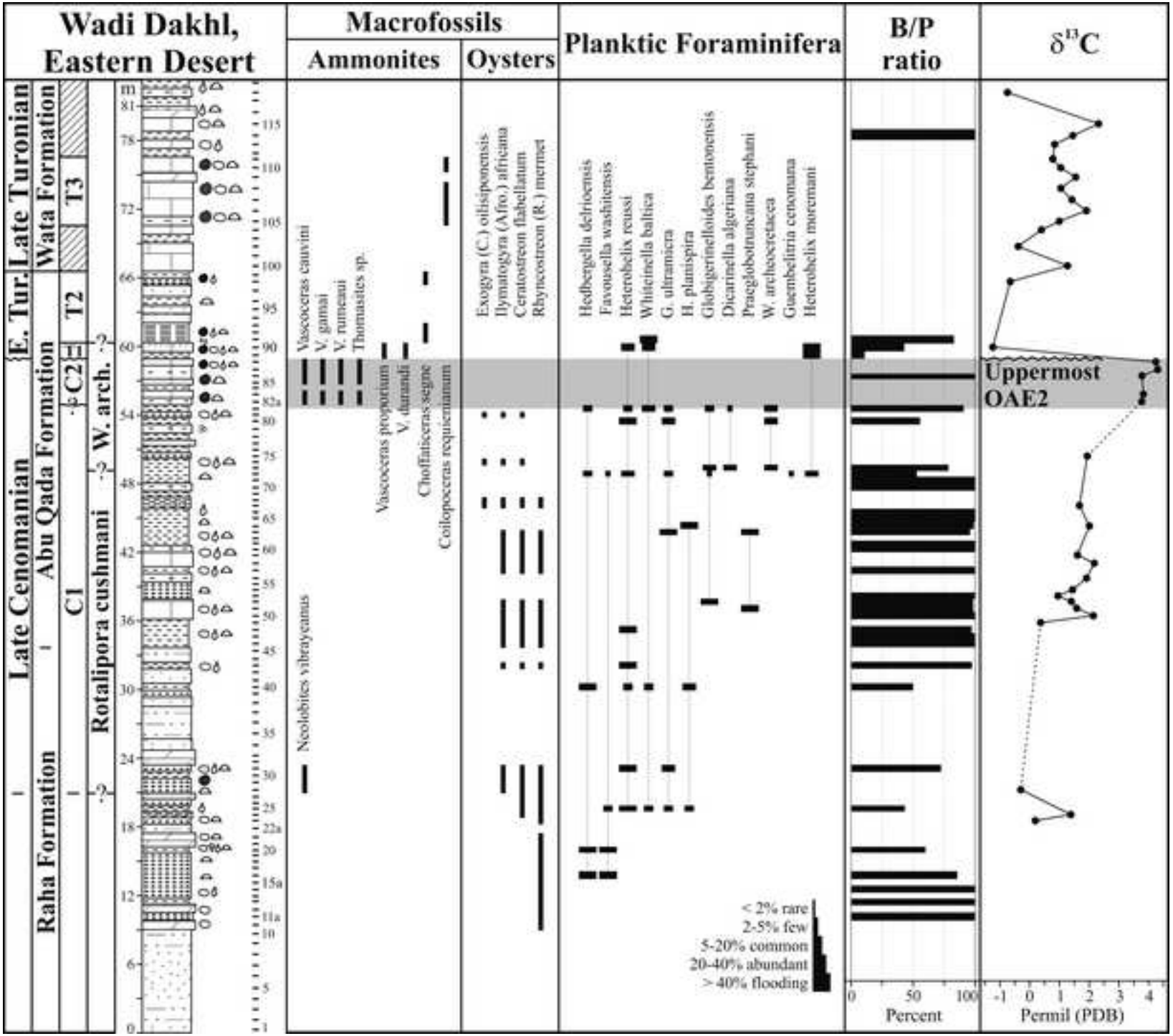

Figure
Click here to download high resolution image

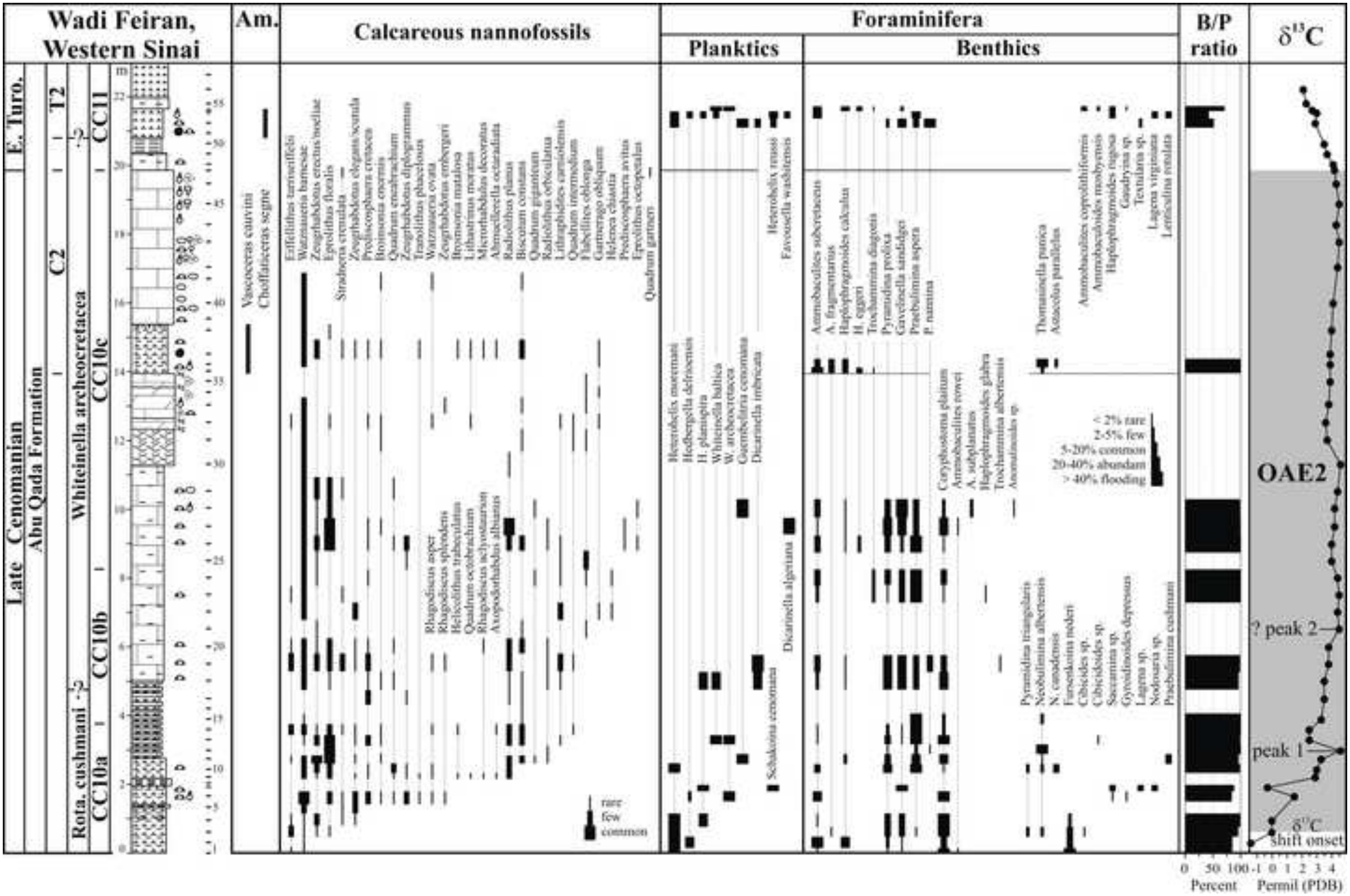

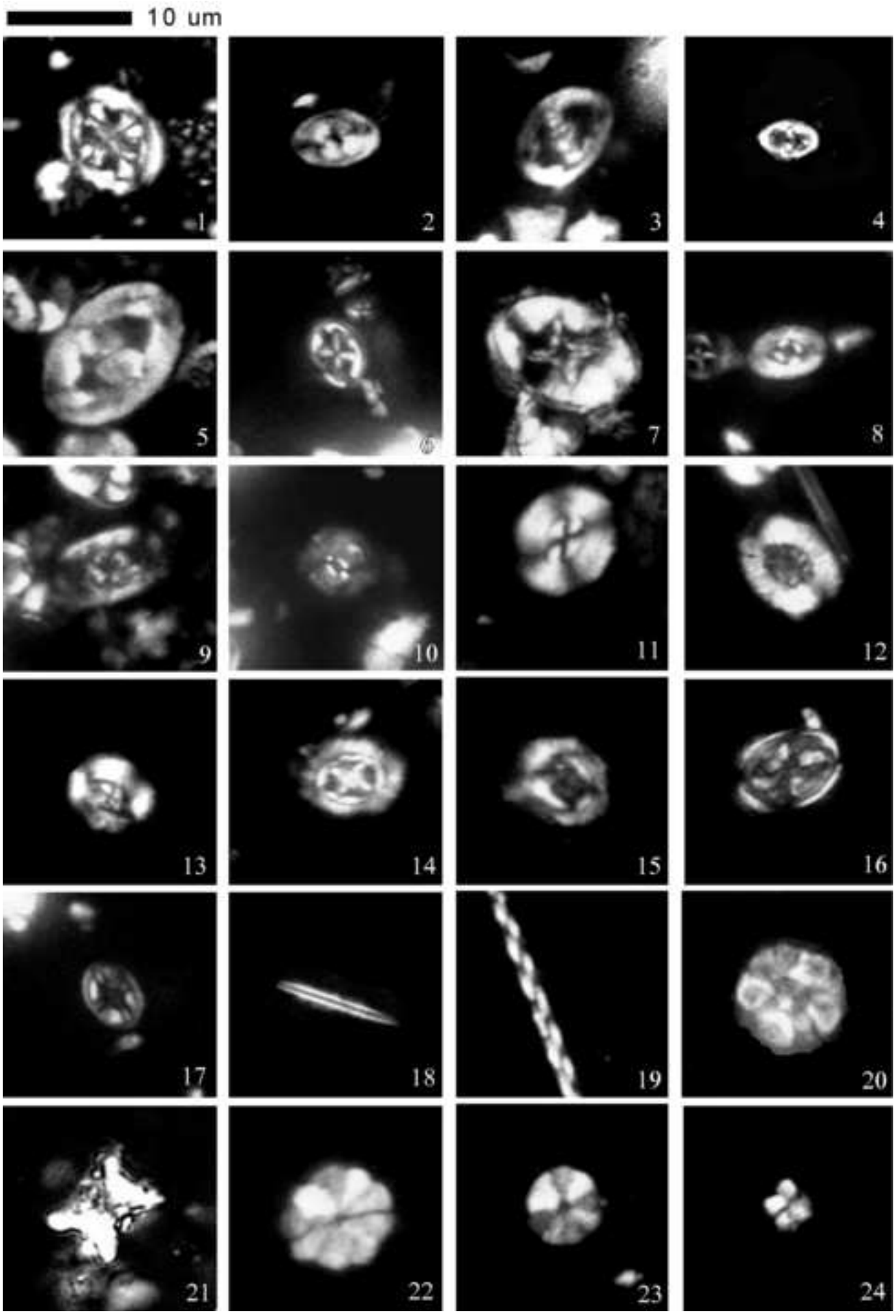

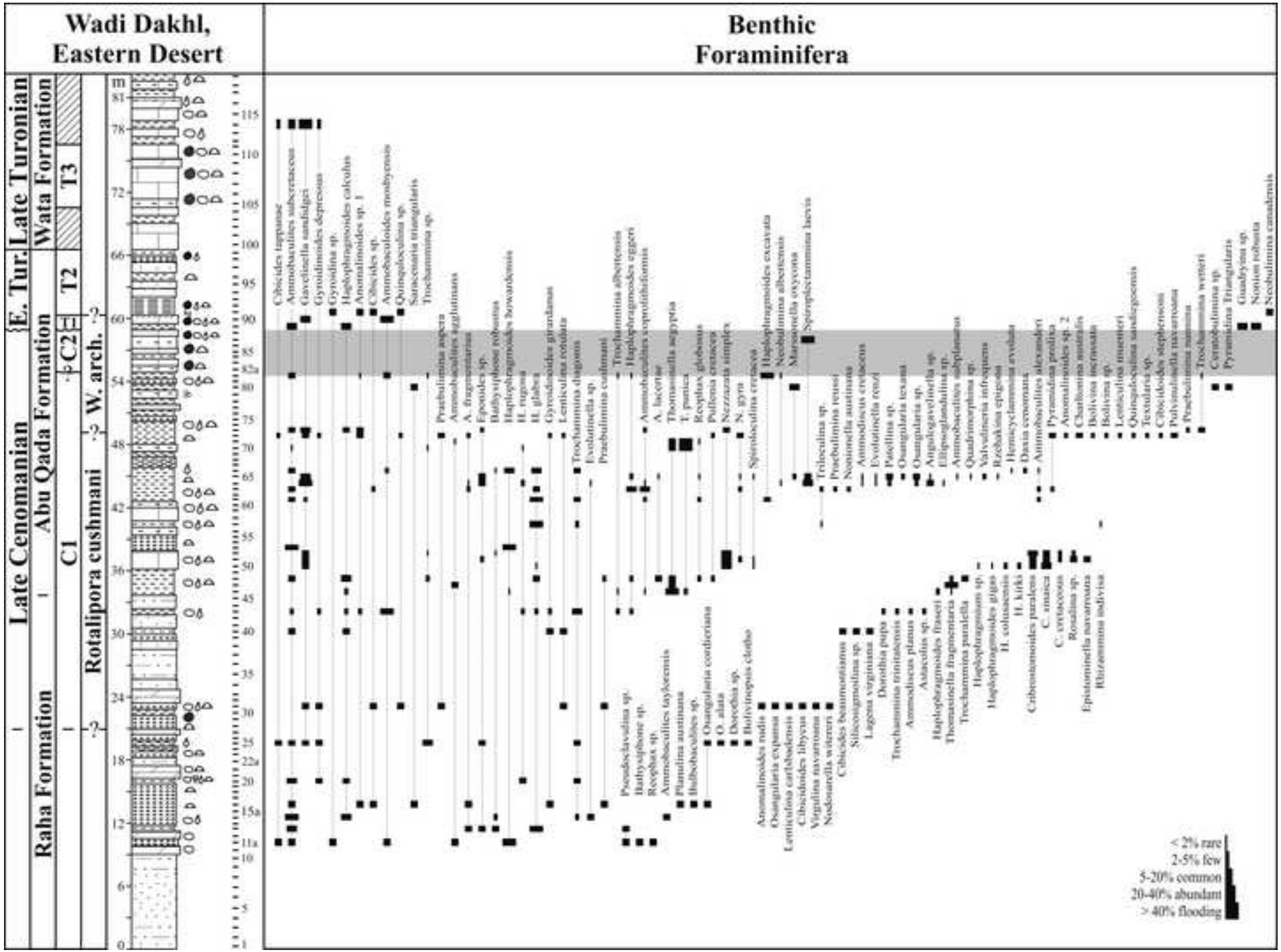

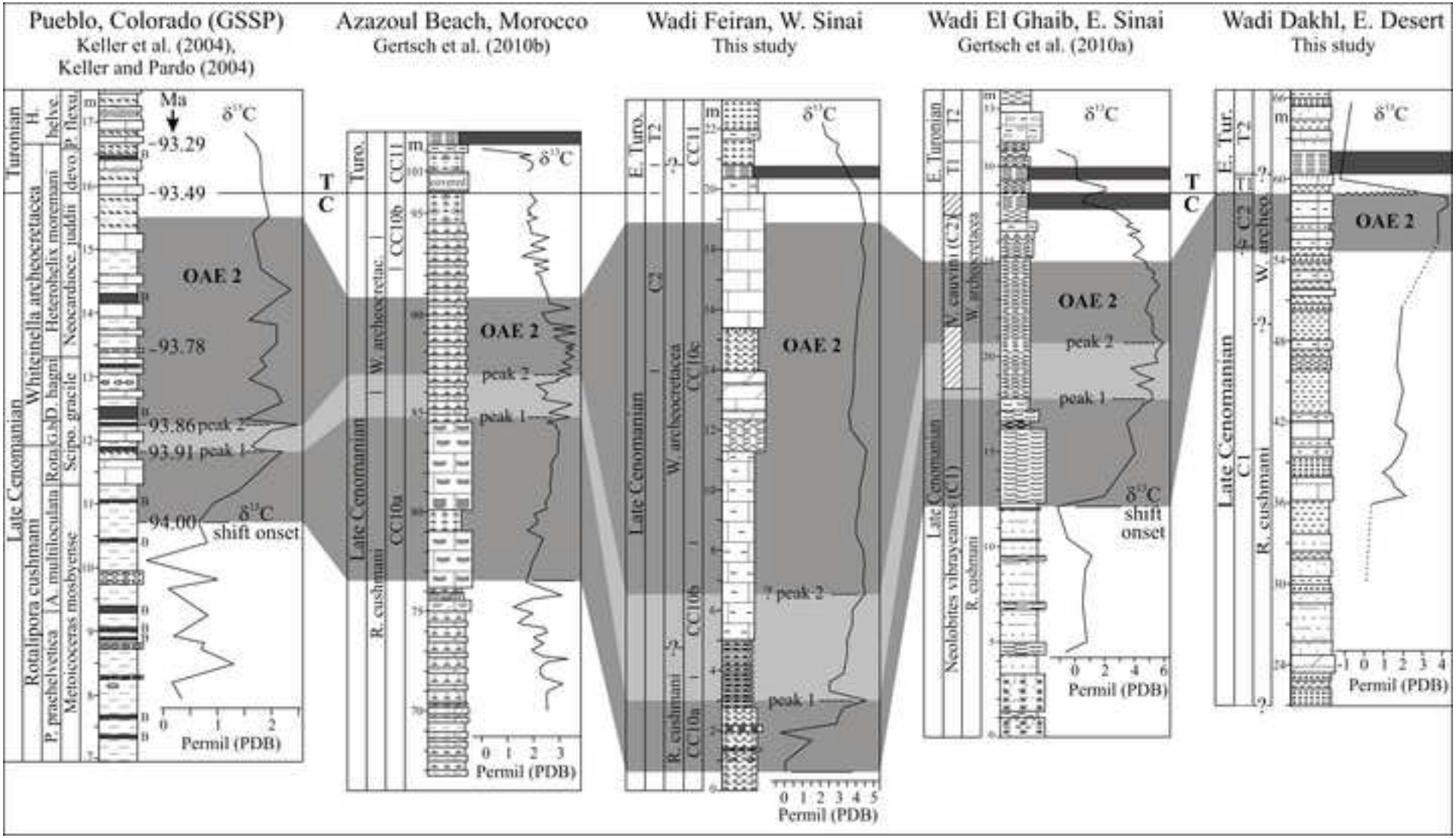

Stage	Western Interior Kennedy et al. (2000)	Europe Hardenbol et al. (1998)	North Africa Caron et al. (2006), Amédro and Robaszynski (2008)	The Middle East Lewy and Raab (1976), Lewy et al. (1984)	Egypt Kassab and Obaidalla (2001), Gertsch et al. (2010a), this study
Early Turonian	*M. nodosoides*	*M. nodosoides*	*M. nodosoides*	*Ch. luciae*	*Ch. segne* (T2)
	V. birchbyi	*W. coloradoense*	*T. rollandi*	*Ch. quaasi* *Ch. securiforme*	
	P. flexuosum		*P. flexuosum*	*V. pioti*	*V. proprium* (T1)
	W. devonense	*W. devonense*	*Watinoceras* sp.		
Late Cenomanian	*N. scotti* *N. juddii*	*N. juddii*	*P. pseudonodosoides*	*V. cauvini*	*V. cauvini* (C2)
	S. gracile	*M. geslinianum*	*M. geslinianum*	*Kanabiceras* sp.	*N. vibrayeanus* (C1)
	M. mosbyense	*C. naviculare/* *E. pentagonum/* *C. guerangeri*	*E. pentagonum*	*Calycoceras* sp.	
	C. canitaurinum			*N. vibrayeanus*